



Universidade do Algarve

Faculdade de Ciências e Tecnologia

# Polyelectrolyte complexes from chitosan and carrageenan: optimization by response surface methodology and method validation

**Rahaf Alsayed**

Dissertação para obtenção do grau de Mestre em Ciências Farmacêuticas

Trabalho realizado sob a orientação da Professora Doutora Ana Maria dos Santos Rosa da Costa e a coorientação da Professora Doutora Ana Margarida Moutinho Grenha

2022-2023



Universidade do Algarve

Faculdade de Ciências e Tecnologia

# Polyelectrolyte complexes from chitosan and carrageenan: optimization by response surface methodology and method validation

**Rahaf Alsayed**

Dissertação para obtenção do grau de Mestre em Ciências Farmacêuticas

Trabalho realizado sob a orientação da Professora Doutora Ana Maria dos Santos Rosa da Costa e a coorientação da Professora Doutora Ana Margarida Moutinho Grenha

2022-2023

# Polyelectrolyte complexes from chitosan and carrageenan: optimisation by response surface methodology and method validation

## **Declaração de autoria de trabalho**

Declaro ser a autora deste trabalho, que é original e inédito. Autores e trabalhos consultados estão devidamente citados no texto e constam da listagem de referências incluída.

**Copyright© 2023 [Rahaf Alsayyed]**

A Universidade do Algarve tem o direito, perpétuo e sem limites geográficos, de arquivar e publicitar este trabalho através de exemplares impressos reproduzidos em papel ou de forma digital, ou por qualquer outro meio conhecido ou que venha a ser inventado, de o divulgar através de repositórios científicos e de admitir a sua cópia e distribuição com objetivos educacionais ou de investigação, não comerciais, desde que seja dado crédito ao autor e editor.

Polyelectrolyte Complexes from chitosan and carrageenan:  
optimization by Response Surface Methodology and method validation

“To make knowledge work productive will be the great management  
task of this century”

**Peter Drucker**

## Acknowledgments

Com imensa gratidão, encerro cinco anos de estudo e dedicação no mestrado integrado em ciências farmacêuticas. Assim, não quero deixar de agradecer a todos que fizeram parte deste percurso, que me motivaram e depositaram confiança em mim.

Em primeiro lugar, envio imensos agradecimentos à minha família; mãe, pai, irmãos, e tia Fátima, pelo amor e apoio incondicional. Apesar da distância que nos separa e que representou o maior desafio nesta jornada, vocês estavam sempre no meu coração. O vosso suporte incessável e persistente permitiu-me aceitar todos os desafios e sempre seguir em frente. Obrigada por não deixarem de acreditar em mim. Obrigada, pai, obrigada mãe, obrigada Ismael, obrigada Kareem... amo-vos muito.

Gostaria também de prestar homenagem à memória do ex-Presidente da República Portuguesa e fundador da plataforma global dos estudantes sírios, o Doutor Jorge Sampaio. Deixo ainda muitos agradecimentos à toda a equipa da plataforma, nomeadamente à Doutora Helena Barroco pelo apoio constante nos passados cinco anos.

Às minhas orientadoras, a Professora Doutora Ana Costa dos Santos e a Professora Doutora Ana Margarida Grenha, quero expressar a minha sincera e profunda gratidão. Agradeço por me terem guiado no mundo de investigação, a área que sempre foi a minha paixão. A vossa orientação era fundamental para crescer e abrir oportunidades.

Professora Ana Costa, obrigada por todo o esforço e orientação mais cedo no primeiro ano de curso, e também neste trabalho. Agradeço por toda a simpatia, devoção, e apoio que demonstrou! Também pelas longas horas de explicações sem se cansar de tirar as minhas dúvidas. A minha paixão pela química orgânica despertou-se nas suas aulas, e continua a crescer até agora. Tenho muito mais por dizer, mas as palavras não chegam para lhe agradecer.

Professora Ana Grenha, a sua dedicação à investigação e ciência sempre foi inspiradora para mim. Consigo aprendi a determinação e desenvolvi amor pelos manipulados. As aulas da tecnologia farmacêutica acompanharam-me durante todo o estágio, e sem essas aulas, o estágio não teria sido tão eficaz como foi. Agradeço-lhe todo o apoio e a orientação desde o início até agora.

A todos os meus professores e professoras que se dedicaram a nos ao longo dos cinco anos de curso, uma grande obrigada. Ao Professor Américo Lemos e à Professora Maria de Lurdes Cristiano, e mais uma vez à Professora Ana Costa, obrigada por incutirem o amor pela química orgânica que é a primeira porta a ser aberta para entrar no mundo das ciências farmacêuticas. Professora Maria de Lurdes, terei sempre saudades das suas aulas, e nunca deixarei “de olhar para a estrutura de molécula”.

À Professora Isabel Ramalhinho, um agradecimento enorme por tudo; pela simpática e pelo apoio incansável durante o estágio e, também, o curso. Tive a sorte de tê-la como tutora de estágio. Agradeço por todos os telefonemas a perguntar como estava a correr o estágio. Obrigada por estar sempre aqui para ajudar nos momentos menos agradáveis.

Aos locais do estágio, obrigada pelo acolhimento e amizade. Obrigada à equipa da farmácia Estácio, nomeadamente à Susana, Ana, Francisca e João. Aprendi muito convosco. Obrigada à

Polyelectrolyte Complexes from chitosan and carrageenan:  
optimization by Response Surface Methodology and method validation

equipa do laboratório dos estudos farmacêuticos. Obrigada, Florbela, Francisco, Beatriz, Ana, Carolinas e Diana.

Aos amigos e colegas que partilharam risos, momentos de estudo e apoio mútuo, obrigada.

Aos colegas no laboratório do Drug Delivery, obrigada. Obrigada, Jorge e Noélia!

À minha amiga Mona, obrigada por me aturares nos momentos menos bons e por estares sempre aqui para me ouvir.

Ao professor Rui Cruz, envio os meus sinceros agradecimentos pela assistência e ajuda em tudo que toca o desenho experimental.

E finalmente, aos meus colegas na farmácia Sacoor, obrigada por toda a resiliência e ajuste de horários que me ajudou dedicar à dissertação. Joana, a tua colaboração é bastante apreciada.

## Abstract

Polyelectrolyte complexes (PECs) are important emerging materials in the pharmaceutical industry, especially because they are easily prepared in mild conditions, devoid of organic solvents and other harsh conditions. So far, a large number of scientific articles has been published reporting the possible applications of PECs as drug carriers. Polyelectrolytes own unique features, as they join the properties of polymers and electrolytes. These features turn PECs sensitive to the surrounding environment, such as salt concentration, that can considerably alter their formation and characteristics. Therefore, this work encompassed establishing an experimental design to optimize the formation of PECs from two polyelectrolytes, chitosan (CS) and carrageenan (CRG), in the absence and presence of NaCl in different concentrations.

For that, preliminary studies were conducted to determine the solubility of CS and CRG in NaCl solutions, as well as the isoelectric point of PECs. Afterwards, an experimental design was established using response surface methodology to predict the size and zeta potential of the PECs, as well as the yield (measured as turbidity) of the obtained colloid. The design was constructed over a range of CS, CRG and NaCl concentrations that varied from 0 to 2 mM, 0 to 1.67 mM, and 0 to 0.06 M, respectively.

Response surfaces and contour diagrams that represent the variations of size and zeta potential with the variation of the concentrations of CS, CRG and NaCl were obtained. Under the tested conditions, nanoparticles ranging in 280 - 700 nm and showing  $\pm 49$  mV of zeta potential were obtained. The design was later validated and was found to predict with high desirability the size and zeta potential of PECs, but unfortunately failed to predict the yield.

As a conclusion, PECs formation from CS and CRG in NaCl solutions can be optimized using the experimental design from this study, which resulted in a model that can predict with high credibility the conditions leading to the formation of particles with specific size and zeta potential.

Keywords: Carrageenan, Chitosan, Experimental design, Polyelectrolyte complexes, Response surface methodology

## Resumo

Os complexos polieletrólíticos (PECs) têm vindo a ganhar uma enorme visibilidade na indústria farmacêutica nos últimos anos. Os PECs destacam-se pela fácil preparação, que dispensa o uso de solventes orgânicos. Existem inúmeros artigos na literatura que reportam a aplicabilidade dos PECs na área de veiculação de fármacos, pois devido às características únicas dos polieletrólitos, que reúnem as propriedades de polímeros e eletrólitos, estes compostos terão elevado potencial nesta área. Estas características tornam os PECs altamente sensíveis às características do meio, como por exemplo a força iónica. Sendo assim, procedeu-se neste trabalho à construção de um desenho experimental a fim de otimizar a formação de PECs de quitosano (CS) e carragenina (CRG), na presença e ausência de NaCl de diferentes concentrações.

Com esse objetivo, realizaram-se estudos preliminares para determinar a solubilidade do CS e da CRG em soluções de NaCl, bem como o ponto isoelétrico dos PECs. Posteriormente, construiu-se um desenho experimental recorrendo à metodologia de superfície de resposta a fim de prever o tamanho, o potencial zeta, e o rendimento dos PECs, medido através da turbidez do colóide. As concentrações mínimas e máximas dos componentes do desenho são 0 - 2 mM, 0 - 1,67 mM, e 0 - 0,06 M de CS, CRG, e NaCl, respetivamente.

Obtiveram-se superfícies de resposta assim como diagramas de contorno a partir do desenho experimental. Estes representam as variações do tamanho e do potencial zeta com as variações dos três parâmetros, concentrações de CS, CRG e NaCl. Nas condições estudadas, obtiveram-se PECs de tamanhos que variam entre 280 e 700 nm e potencial zeta de  $\pm 49$  mV. Procedeu-se, depois, à validação do desenho. O mesmo comprovou-se válido e capaz de prever o tamanho e o potencial zeta dos PECs com alta desejabilidade. No entanto, não se comprovou válido em fazer previsões do rendimento de preparação do colóide.

Concluiu-se que se pode otimizar a formação dos PECs de CS e CRG em soluções de NaCl usando o desenho experimental desenvolvido neste estudo, e que este desenho pode prever as condições que permitem a formação de PECs de tamanho e potencial zeta específicos.

Palavras-chave: Carragenina, Complexos polieletrólíticos, Desenho Experimental, Quitosano, Superfícies de resposta

## Resumo alargado

Os complexos polieletrólitos (PECs) têm vindo a ganhar grande visibilidade na indústria farmacêutica nos últimos anos devido ao seu grande potencial em diversas aplicações biomédicas e farmacêuticas, sobretudo na tecnologia farmacêutica e na área da veiculação de fármacos. Os exemplos mais relevantes dizem respeito a estudos que indicam que os PECs terão grande potencial de aplicação no desenvolvimento de terapia individualizada dos tumores malignos, e nas estratégias de vacinação. Os PECs têm, igualmente, um papel não desprezável no combate contra as resistências microbianas aos antimicrobianos, já que alguns destes fármacos se podem complexar com polieletrólitos (PEs). Além disso, existem PECs com propriedades antimicrobianas próprias.

De facto, os PECs resultam da complexação entre dois PEs de cargas opostas ou entre um PE e uma substância ativa tendo aqui como exemplo a complexação com o ácido ribonucleico (RNA), salientando, assim, a importância dos PECs nas áreas da vacinação e da terapia génica. Os PEs de origem natural ou sintética podem entrar na composição dos PECs, entretanto, comprovou-se que os primeiros têm um potencial muito mais alto nas aplicações médicas e farmacêuticas graças a um conjunto de propriedades tal como a sua potencial biocompatibilidade, biodegradabilidade e baixa toxicidade.

Hoje em dia, fala-se muito da química verde e do desenvolvimento de alternativas menos prejudiciais para o meio ambiente. Na verdade, os PECs destacam-se de outros veículos de fármacos, tal como lipossomas ou até outras nanopartículas poliméricas, por serem de fácil preparação, que dispensam o uso de solventes orgânicos, tendo a água como solvente base na sua preparação.

Existem inúmeros artigos na literatura que reportam a aplicabilidade dos PECs na área de veiculação de fármacos, pois devido às características únicas dos PEs que reúnem as propriedades de polímeros e eletrólitos na mesma molécula, os investigadores acreditam que estes materiais terão um grande potencial nesta área. No entanto, estas mesmas características tornam os PECs menos estáveis nalgumas condições e muito sensíveis às condições do meio, como por exemplo a acidez (pH) e a força iónica. Deve-se ter em consideração essa sensibilidade dos PECs, uma vez que a força iónica dos fluidos corporais pode influenciar a estabilidade destes veículos de fármaco *in vivo*, logo, com consequências ao nível do efeito terapêutico.

## Polyelectrolyte Complexes from chitosan and carrageenan: optimization by Response Surface Methodology and method validation

Sendo assim, e tendo em consideração o efeito que os sais possam ter nos PEs e PECs, procedeu-se neste trabalho à otimização da formação de PECs de quitosano (CS), um polícatião extraído de crustáceos, e carragenina (CRG), um polianião obtido de algas vermelhas, em presença e na ausência de NaCl.

Para tal, realizaram-se estudos preliminares com o objetivo de delimitar as concentrações de sal e polímeros a utilizar no estudo. Realizou-se o primeiro estudo com o propósito de selecionar, de entre várias carrageninas comerciais, a mais adequada para a formação dos PECs. Esse ensaio permitiu avaliar o efeito da concentração da CRG nas características dos PECs, tal como o potencial zeta e o tamanho. Comprovou-se que o aumento da concentração de CRG se reflete num aumento do tamanho dos PECs, mas não tem efeito no potencial zeta.

O segundo estudo preliminar teve como objetivo determinar a solubilidade de cada um dos PEs em soluções de três sais: NaCl, CaCl<sub>2</sub> e Na<sub>2</sub>SO<sub>4</sub>. Verificou-se que a solubilidade dos PEs é menor em Na<sub>2</sub>SO<sub>4</sub>, seguindo-se o CaCl<sub>2</sub> e é maior em NaCl.

O último estudo preliminar foi realizado com o fim de determinar o ponto isoelétrico dos PECs. Nesse ponto, o potencial zeta dos PECs é zero, assim, a carga total do sistema é zero. Estimou-se que se atinge o ponto isoelétrico numa formulação com a composição aproximada de 5,75/1, correspondente a  $n^-/n^+ \approx 3,5$ .

Baseando-nos nos resultados dos estudos preliminares e em resultados obtidos em trabalhos anteriores, construiu-se um desenho experimental de tipo *mixture experiment* com 3 componentes: concentrações de CS, CRG e NaCl. O desenho comprovou ter capacidade de prever as concentrações a utilizar para obter PECs com determinadas características de tamanho e potencial zeta com alta desejabilidade.

O desenho é constituído por 15 pontos experimentais com as seguintes concentrações mínimas e máximas: CS: 0 - 66,67%, CRG: 0 - 66,67%, e NaCl: 0 - 60%. Os PECs obtidos foram caracterizados quanto ao tamanho e potencial zeta, tendo-se ainda medido a turbidez do colóide. Obtiveram-se as superfícies da resposta correspondentes ao tamanho e potencial zeta.

Posteriormente, efetuou-se a validação do desenho experimental, tendo-se preparado cinco réplicas de três pontos selecionados do desenho que permitem uma previsão com alta desejabilidade. Os pontos correspondem às formulações com potencial zeta de -49 mV, +49 mV e tamanho de 284 nm.

O desenho experimental comprovou-se válido, uma vez que resulta em valores muito próximos daqueles obtidos experimentalmente. Concluiu-se que se pode otimizar a formação

dos PECs de CS e CRG em presença de NaCl usando o desenho experimental desenvolvido neste estudo, e que este desenho pode prever as condições que permitem a formação de PECs de tamanho tão pequeno quanto 284 nm e potencial zeta de  $\pm 49$  nm, valores promissores em muitas aplicações farmacêuticas. Mesmo assim, estudos futuros serão imprescindíveis na otimização dos PECs tendo em conta outros parâmetros como, por exemplo, o peso molecular do polímero e a temperatura do meio da reação, entre outros, uma vez que estudos anteriores comprovaram a importância destes parâmetros na formação e propriedades dos PECs. Para além disso, pode-se optar por CS com diferentes graus de desacetilação e comparar as diferenças que se reflitam na formação dos complexos.

Por fim, concluiu-se que se pode desenvolver uma ferramenta a partir do desenho desenvolvido neste estudo e que essa é promissora para a futura otimização da formação dos PECs em meio académico ou industrial.

## Table of contents

<b>Abstract.....</b>	<b>V</b>
<b>Resumo.....</b>	<b>VI</b>
<b>Resumo alargado.....</b>	<b>VII</b>
<b>Table of contents .....</b>	<b>X</b>
<b>Figures index .....</b>	<b>XII</b>
<b>Tables index.....</b>	<b>XIV</b>
<b>List of abbreviations .....</b>	<b>XV</b>
<b>1 Introduction.....</b>	<b>1</b>
<b>1.1 Nanotechnology and health.....</b>	<b>1</b>
1.1.1 Polymer-based NPs (PbNP).....	5
<b>1.2 Polyelectrolytes.....</b>	<b>9</b>
1.2.1 Chitosan .....	10
1.2.2 Carrageenan .....	11
<b>1.3 Polyelectrolyte complexes (PECs) .....</b>	<b>13</b>
1.3.1 Characterisation of PECs .....	14
1.3.1.1 Zeta potential .....	14
1.3.1.2 Size.....	16
1.3.2 Mechanisms of formation of PECs .....	17
1.3.3 Factors that affect PECs formation .....	20
1.3.3.1 pH effect.....	21
1.3.3.2 Ionic strength effect .....	22
<b>1.4 Response surface methodology (RSM).....</b>	<b>24</b>
<b>2 Objectives.....</b>	<b>26</b>
<b>3 Materials and methods .....</b>	<b>27</b>
<b>3.1 Materials .....</b>	<b>27</b>
<b>3.2 Preparation and characterisation of PECs from commercial CS and CRG....</b>	<b>27</b>

Polyelectrolyte Complexes from chitosan and carrageenan:  
optimization by Response Surface Methodology and method validation

<b>3.3</b>	<b>Purification of PEs .....</b>	<b>28</b>
<b>3.4</b>	<b>Precipitation study, determining the solubility of PEs in salt solutions.....</b>	<b>28</b>
<b>3.5</b>	<b>Determining the isoelectric point (IP) .....</b>	<b>28</b>
<b>3.6</b>	<b>Construction of the Experimental Design (ED) .....</b>	<b>30</b>
<b>3.7</b>	<b>Method validation .....</b>	<b>32</b>
<b>3.8</b>	<b>Statistical analysis .....</b>	<b>32</b>
<b>4</b>	<b>Results and discussion .....</b>	<b>34</b>
<b>4.1</b>	<b>Preparation and characterisation of PECs from commercial CS and CRG....</b>	<b>34</b>
<b>4.2</b>	<b>Precipitation study, determining the solubility of PECs in salt solutions.....</b>	<b>37</b>
<b>4.3</b>	<b>Determining the isoelectric point (IP) .....</b>	<b>39</b>
<b>4.4</b>	<b>Constructing the Experimental Design (ED).....</b>	<b>42</b>
<b>4.5</b>	<b>Method validation .....</b>	<b>46</b>
<b>5</b>	<b>Conclusion .....</b>	<b>48</b>
<b>6</b>	<b>References .....</b>	<b>49</b>
<b>7</b>	<b>Annexes .....</b>	<b>60</b>

## Figures index

Figure 1.1 - Dimensions of some organs, creatures, and molecules highlighting how small the nanoscale is and the applicability of nanomaterials. Adapted from (6).	1
Figure 1.2 - The advantages of NPs in comparison to microparticles in cellular internalisation. A NP enters, while a microparticle does not. Adapted from (29).	4
Figure 1.3 - Classification of NPs into three main categories. Adapted from (32).	5
Figure 1.4 - Classification of polymer-based NPs. Adapted from (34).	6
Figure 1.5 - The structure of RNA, a polyanion. Adapted from (50).	9
Figure 1.6 - The chemical structure of CS, composed of D-glucosamine (right) and N-acetyl-D-glucosamine (left) units. Adapted from (59).	10
Figure 1.7 - The structure of $\kappa$ -CRG composed of 1,3 $\beta$ -D-galactose (left) 1,4 anhydrogalactose (right) units. Adapted from (68).	12
Figure 1.8 - Electric double layer. Adapted from (97).	16
Figure 1.9 - The formation of soluble PECs: there is a large host PE and a small guest PE. Adapted from (101).	18
Figure 1.10 - Ladder (a) and scrambled egg (b) structures of PECs. Adapted from (107).	19
Figure 1.11 - PECs formation can be endothermic or exothermic according to salt concentration. $\Delta F$ : the total free energy of the complexation reaction, $-T \Delta S$ : counterion release entropy, $\Delta E$ : Coulomb energy. Adapted from (51).	20
Figure 1.12 - Factors that influence PECs formation. Adapted from (112).	21
Figure 1.13 - The effect of pH on PECs from CS and heparin. Adapted from (115).	22
Figure 1.14 - The effect of NaCl on the formation of nanoplexes from ciprofloxacin (CIP) and a PE. Adapted from (89).	23
Figure 3.1 - The process of PECs formation (1 and 2) and characterisation (3). 1: preparing the PEs solutions, 2: adding CRG to CS solution, and 3: characterisation using Zetasizer (a) and Spectrophotometer (b).	31
Figure 4.1 – Effect of CS/CRG mass ratios on the size of PECs produced with CS and CRG from Biopolymer (blue line) and Sigma (orange line); Formulation 2/1 Sigma precipitated (mean $\pm$ SD, n = 3).	36
Figure 4.2 – Effect of CS/CRG mass ratios on the polydispersity index (PDI) of PECs produced with CS and CRG from Biopolymer (blue line) and Sigma (orange line); Formulation 2/1 Sigma precipitated (mean $\pm$ SD, n = 3).	36

Polyelectrolyte Complexes from chitosan and carrageenan:  
optimization by Response Surface Methodology and method validation

Figure 4.3 - Effect of CS/CRG mass ratios on the zeta potential (ZP) of PECs produced with CS and CRG from Biopolymer (blue line) and Sigma (orange line); Formulation 2/1 Sigma precipitated (mean  $\pm$  SD, n = 3).....37

Figure 4.4 - Variation of zeta potential (ZP) values of PECs from CS and CRG with charge ratio ( $n^-/n^+$ ); From 1.80 to 4,33 precipitation was noticed and ZP was not measured. ....40

Figure 4.5 - The mechanism of PECs formation from CS and CRG.....40

Figure 4.6 - Variation of transmittance (%T) of PECs from CS and CRG with charge ratio ( $n^-/n^+$ ).....42

Figure 4.7 - Response surface (a) and contour diagram (b) of size. ....43

Figure 4.8 - Response surface (a) and contour diagram (b) of zeta potential (ZP).....45

## Tables index

Table 3.1 - Concentrations of CS and CRG and $n^-/n^+$ ratios used to determine the isoelectric point of PECs. Formulations $n^-/n^+ = 1.80 - 4.33$ precipitated (*). .....	29
Table 3.2 - Points selected from ED4 for validation. Desirability = 1 for all the predicted values. ....	32
Table 4.1 - NaCl, CS, and CRG concentrations at which precipitation happens. ....	38
Table 4.2 - Size, polydispersity index (Pdl), zeta potential (ZP), and count rate (CR) values of PECs prepared for method validation (mean $\pm$ SD, n = 5). ....	46
Table 7.1 - Concentrations of CS, CRG, and NaCl used to construct the ED1, in addition to the corresponding Size, ZP, %T, and Count Rate readings; measurement was done (-). .....	60
Table 7.2 - Concentrations of CS, CRG, and NaCl used to construct the ED2, in addition to the corresponding Size, ZP, %T, and Count Rate readings; measurement was done (-), precipitation happened (-). ....	60
Table 7.3 - Concentrations of CS, CRG, and NaCl used to construct the ED3, in addition to the corresponding Size, ZP, %T, and Count Rate readings; measurement was done (-), precipitation happened (*). ....	61
Table 7.4 - Concentrations of CS, CRG, and NaCl used to construct the ED3, in addition to the corresponding Size, ZP, %T, and Count Rate readings. ....	62

## List of abbreviations

**AFM** - Atomic force microscopy

**ANOVA** - Analysis of variance

**COVID-19** - Coronavirus disease 19

**CR** - Count Rate

**CRG** - Carrageenan

**CS** - Chitosan

**DLS** - Dynamic light scattering

**DNA** - Deoxyribonucleic acid

**ED** - Experimental design

**ELS** - Electrophoretic light scattering

**FDA** - Food and Drug Administration

**HIV** - Human Immunodeficiency virus

**HPV** - Human papilloma virus

**HSV** - Herpes simplex virus

**IP** - Isoelectric point

**mRNA** - messenger ribonucleic acid

**NP** - Nanoparticle

**PbNP** - Polymer-based nanoparticles

**PE** - Polyelectrolyte

**PEC** - Polyelectrolyte complex

**PEG** - polyethylene glycol

**RNA** - Ribonucleic acid

**ROS** - Reactive oxygen species

**RSM** - Response surface methodology

**SARS-COV-2** - Severe acute respiratory syndrome-coronavirus-2

**SD** - Standard deviation

**TEM** - Transmission electron microscopy

**UV-Vis** - Ultraviolet-visible

**ZP** - Zeta potential

# 1 Introduction

## 1.1 Nanotechnology and health

Nanotechnology is the study and application of materials at dimensions in the nanometer range, typically between 1 and 100 nm. At these dimensions, the matter starts acquiring different chemical, physical, mechanical, and optical properties responsible for the wide applications in diverse sectors, such as industries, pharmacy, medicine, information technology, and environmental sciences, like water treatment (1–4). However, it is noteworthy that for pharmaceutical and medical applications, matter of dimensions below 1000 nm are still considered to be under the umbrella of nanotechnology (5). **Figure 1.1** illustrates a comparison between the sizes of different body parts, organelles, and molecules, which facilitates understanding how small the nanoscale is (6).

The unique features that nanomaterials possess are not only due to their small size, a property that allows those materials to extravasate and reach very specific sites in the cell compartments, thereby reducing side effects (4,7), but also due to the high surface-to-volume ratio. Imagine that a cube of 1 cm<sup>3</sup> is divided into cubes of 1 nm<sup>3</sup>, the total surface of those covers more than a football field; a considerably high surface compared to the volume, which renders those materials more reactive (3,8).

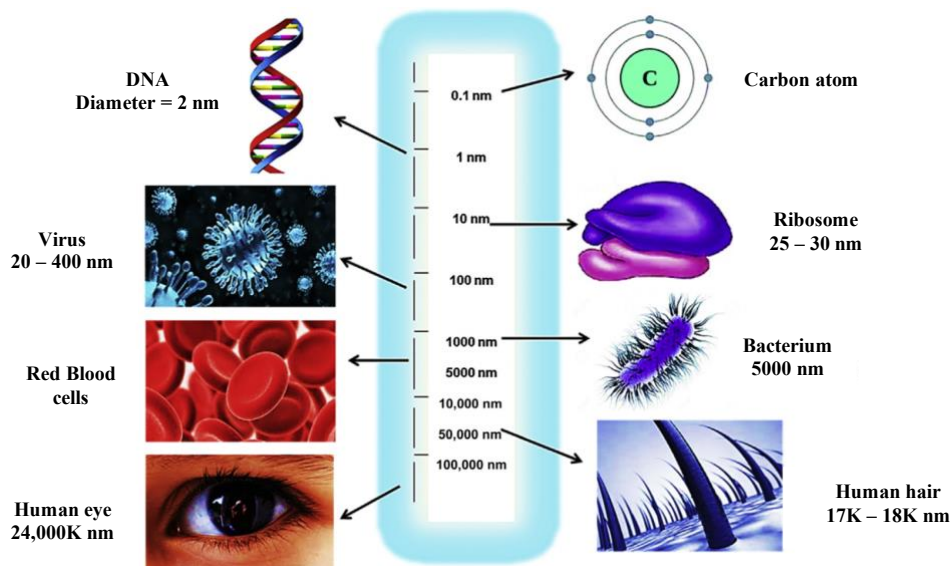


Figure 1.1 - Dimensions of some organs, creatures, and molecules highlighting how small the nanoscale is and the applicability of nanomaterials. Adapted from (6).

## Polyelectrolyte Complexes from chitosan and carrageenan: optimization by Response Surface Methodology and method validation

Nanomedicine is a recently emerging branch of nanotechnology. It refers to the application of nanomaterials to cure, prevent, and diagnose diseases. That implies using nanotechnology-based systems such as nanoparticles and nanorobots for those ends (9,10). Drug delivery has a big share of nanomedicine applications, as according to a 2008 report from the European Commission, 76% of nanomedicine publications were on topics related to drug delivery. Furthermore, drug delivery had the share of 59% of patents (11). In addition, the size of nanotechnology drug delivery global market was about 84 billion dollars in 2022 and is expected to have a high growth rate reaching 183.11 billion dollars in 2032 (12).

Nanoparticles (NPs) are very commonly used drug delivery systems on the nanoscale, and their importance increases owing to the possibility of being functionalised. Hence, NPs can increase drugs' bioavailability by increasing their solubility and providing protection from enzymatic degradation (sheltering the drug), and by providing sustainable release of the encapsulated drugs. Also, surface coating of NPs with hydrophilic molecules such as some types of polyethylene glycol (PEG) increases their half-lives and improves their bioavailability by helping the particles escape the immune system (7).

Nanotechnology has much to offer to many health-related domains. Cancer therapy is one of the best examples where nanotechnology has contributed significantly. Cancer is the second leading cause of death worldwide as 19.3 million new cancer cases and roughly 10 million cancer-caused deaths were estimated in 2020 alone (13). Having that said, the use of nanotechnology in cancer will be indispensable. Due to the unique features of NPs like coating, functionalisation, controlled release, and targeting properties, they gave hope to cancer treatment and diagnosis reducing the debilitating toxic effects of traditional cancer therapy. Increasing drug solubility is an important advantage NPs have offered to cancer chemotherapy, as the vast majority of antitumoral drugs are hardly dissolved in water (10). Due to the above-mentioned properties, nanotechnology gave also new hope to treating cancer with hyperthermia, that is, increasing tumoral tissue temperature to 41- 46 °C without harming other body compartments. Functionalized magnetic NPs such as iron oxide ( $\text{Fe}_3\text{O}_4$ ) NPs are a leading example of particles used in hyperthermia therapy to target tumour site(s). Interestingly,  $\text{Fe}_3\text{O}_4$  NPs can simultaneously carry antitumoral(s) directly to the tumour site. Furthermore, covering those NPs with polymers or other molecules such as PEG or aminosilane to turn them biocompatible has proven to be more effective and less toxic in many *in vitro* and *in vivo* experiments against different types of cancer (14,15).

## Polyelectrolyte Complexes from chitosan and carrageenan: optimization by Response Surface Methodology and method validation

Up to now, there are 100 nanomedicines on the market, of which 15 are for cancer therapy (16,17). Doxil<sup>®</sup> (Caelyx<sup>®</sup> in Europe) is the leading example and is approved to be used in the treatment of ovarian cancer and acquired immunodeficiency syndrome (AIDS)-related Kaposi's sarcoma. It is a liposomal pegylated form of doxorubicin, that has demonstrated lower cardiotoxicity, a problem that hinders clinical applications of doxorubicin, and safer administration of high doses in comparison to the regular doxorubicin, maintaining a high plasma half-life (9,18,19). Moreover, Abraxane<sup>®</sup> is an approved albumin NPs of paclitaxel (Nab-paclitaxel) used in the treatment of breast cancer (9,19), whose goal is to increase the drug's solubility and bioavailability. Nab-paclitaxel has shown many advantages over ordinary paclitaxel, mainly by offering reduced toxicity and increased intra-tumoral concentrations (20). Albumin is normally used in drug carriers due to its biocompatibility and solubility since it is an intrinsic component of the human body. Moreover, it accumulates easily in tumours (21).

NPs have the potential to overcome multidrug resistance caused by the overexpression of ATP-binding cassette (ABC) transporters on cancer cells, mainly p-glycoprotein, which is a huge obstacle faced in cancer therapy (21,22), and also help in targeting multi-drug resistant cells to undergo apoptosis (7).

Besides cancer, nanotechnology has many applications in other fields of health such as tissue engineering, for example. In this context, they are used to improve knee prosthetics, and in bone and tooth repair, benefiting from their aforementioned high strength-to-weight and also antimicrobial properties since NPs can either function as carriers of antibiotics or have, themselves, antimicrobial properties once they disrupt biofilms formation (4,8,23). Carbon-based and metal NPs are the leading examples of NPs with antimicrobial properties and their principal mechanism of action is inducing oxidative stress. In the case of silver NPs, metal ions can be attached to the bacterial cell components leading to metabolism inhibition, damage, and later destruction of the bacterial cell. Other NPs such as lipid and polymer NPs can be loaded with antibiotics such as rifampicin, oxacillin, or rifabutin and have shown great potential in biofilm elimination, especially since they can deliver a high load of antibiotics without causing toxic effects. Furthermore, those NPs can easily penetrate biofilms and can be associated with DNases, enzymes capable of destroying the external matrix of biofilms, facilitating, thus, the reach to bacterial cells and the elimination of biofilms (4,8,23,24). Thanks to their multiple mechanisms of action and large contact surface, NPs have lower chances to provoke resistance if used as antimicrobials. Also, small sizes of NPs help combat intracellular bacteria.

Notwithstanding, some studies found that NPs can have some negative effects on antimicrobial resistance by enhancing plasmid transfer by bacterial conjugation (4).

Moving to viral infections and the important role NPs play in vaccination, the world health organisation (WHO) divulged that 6,943,390 death cases were reported globally due to coronavirus disease 19 (COVID-19) and that the number of cases has sharply decreased after the approval of vaccines against the severe acute respiratory syndrome coronavirus 2 (SARS-COV-2) (25). It is noteworthy that two of those approved vaccines: BioNTech/Comirnaty and Moderna/Spikevax are mRNA vaccines formulated in lipid-based NPs. These NPs could solve some concerns related to vector-based and attenuated vaccines such as the possibility to integrate in the human genome, as well as the possibility to turn pathogenic in the human body, respectively. In addition, lipid-based NPs could confer the necessary protection to mRNA knowing that they are very sensitive to the surrounding environment (26–28).

Compared to microparticles, NPs have huge advantages, as they are considered a good fit for intravenous (IV) delivery. Bearing in mind that capillaries' diameters are 5 - 6  $\mu\text{m}$ , the use of microparticles can lead to capillaries blockage (7). Studies have shown that 100 nm NPs have a 2.5-fold increase in uptake into cellular compartments compared with 1  $\mu\text{m}$  microparticles and 6-fold increase comparing with 10  $\mu\text{m}$  microparticles (**Figure 1.2**) (7,29). An important example refers to NPs used to improve drug access across the blood-brain barrier.

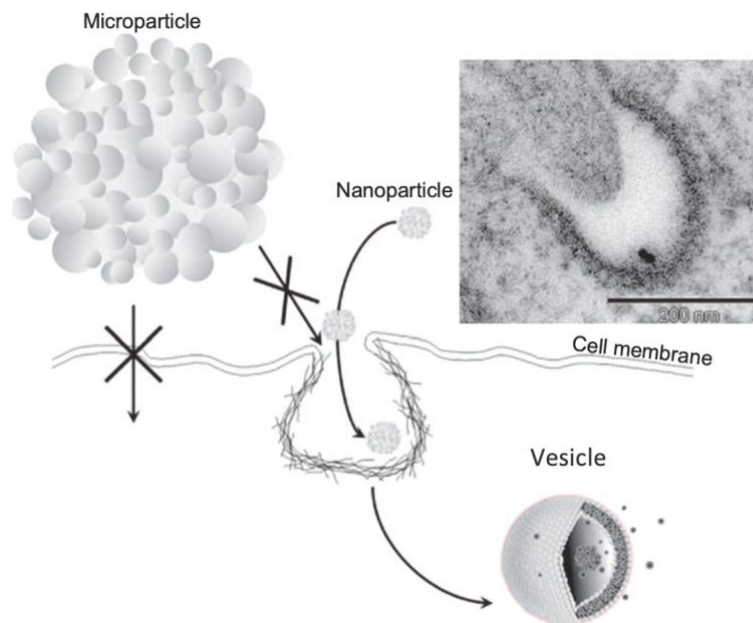


Figure 1.2 - The advantages of NPs in comparison to microparticles in cellular internalisation. A NP enters, while a microparticle does not. Adapted from (29).

Despite the great potential of nanotechnology in providing medical and pharmaceutical solutions, more efforts are still required to investigate those systems, and attention must be paid to other parameters of this technology. The safety of formulations is a relevant aspect, as is the possible environmental hazard, particularly in the case of silver NPs that have antimicrobial activities (9). Interestingly, larger sizes of titanium dioxide ( $\text{TiO}_2$ ) materials did not show to be toxic to humans or the environment, meanwhile, nano  $\text{TiO}_2$  were shown to cause pulmonary damage and sometimes lung cancer in rats. Inside cells, NPs can interfere with chromosomal segregation and lead to DNA alterations, reactive oxygen species (ROS) production, and alterations in metabolic activities; apart from the induction of inflammation (30). Yet, the full image of NPs hazards is not clear and exposure limits are still to be established (27,29).

### 1.1.1 Polymer-based NPs (PbNP)

NPs are classified according to their structure and composition into polymer-based (some authors call them polymeric), lipid-based, and inorganic NPs as depicted in **Figure 1.3** (31,32).

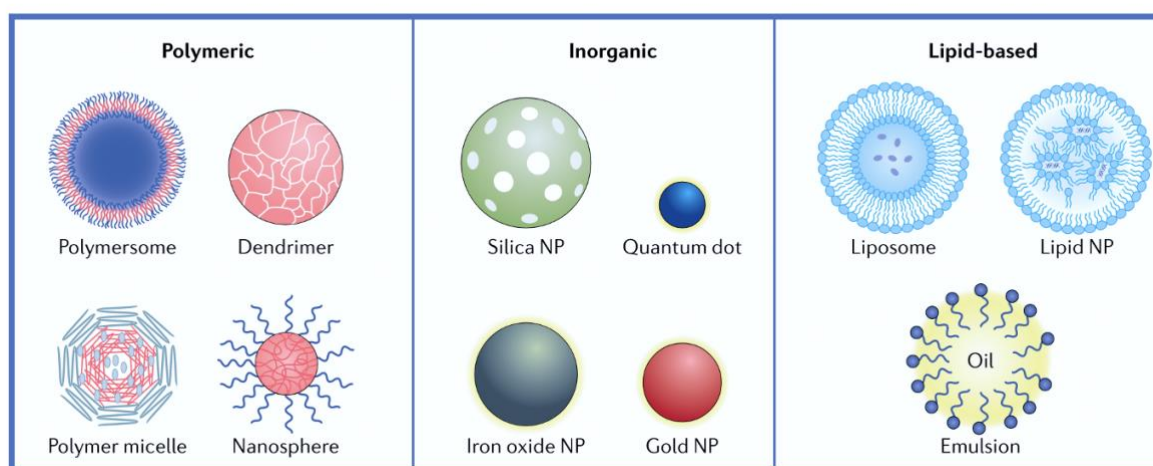


Figure 1.3 - Classification of NPs into three main categories. Adapted from (32).

Those nanosystems are designed to overcome several problems in drug delivery such as drug solubility and drug targeting. Since a big number of drugs approved for clinical applications have low water solubility, those can be carried in PbNP that, in turn, increase their solubility enhancing, therefore, their bioavailability (31). PbNP are composed of either synthetic or natural polymers and their surfaces are functionalizable to target a specific body compartment which leads to obtaining the desired therapeutic results as well as avoiding

adverse effects. The functionalisation of NPs turns them sensitive to the surrounding environment, so that, they release the drug in specific conditions of pH, temperature or oxidation. However, PbNP still pose many challenges regarding aggregation and possible toxic effects, as well as instability and high manufacturing costs which reflects in scaling up difficulties (33).

As shown in **Figure 1.4**, PbNP are versatile as they encompass solid polymeric NPs, micelles, dendrimers, polymersomes, polyplexes, polymer-lipid hybrids, and polymer-drug/protein conjugates (34). They are composed of polymers, and in most cases are nanospheres or nanocapsules with a size varying from 5 nm up to 1000 nm (33). Since PbNP are the focus of our study, below follows a brief description of each existing class.

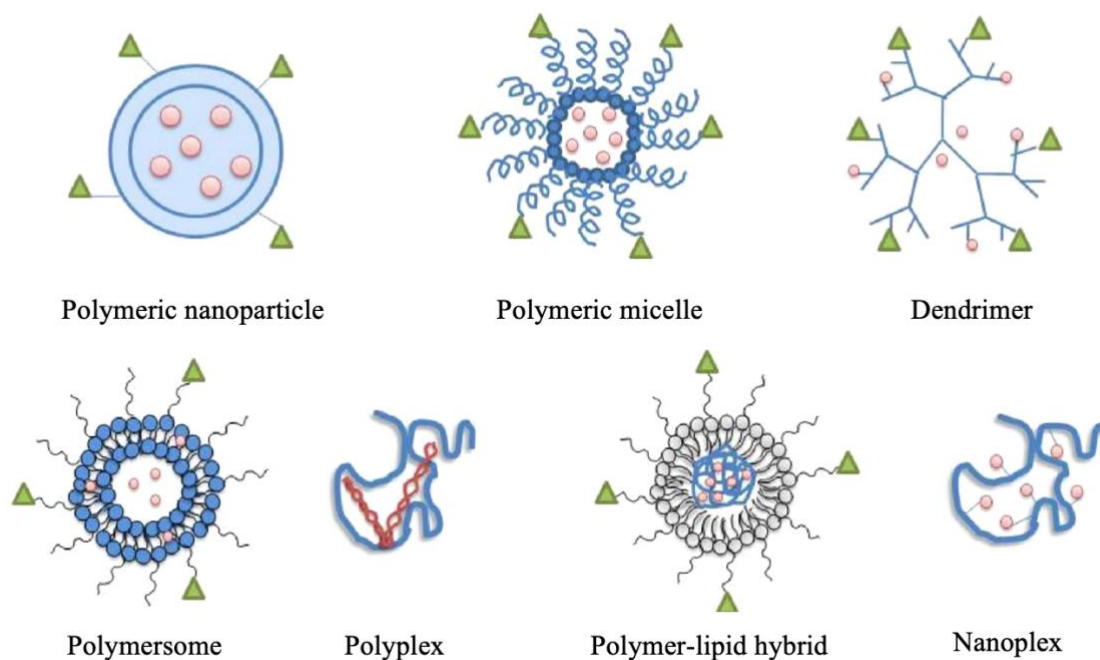


Figure 1.4 - Classification of polymer-based NPs. Adapted from (34).

Polymeric NPs refer to both nanocapsules and nanospheres, where the first comprise a cavity surrounded by a polymeric shell and the second has a continuous matrix of entangled polymers. There are several methods applied in the preparation of polymeric NPs. The starting materials can either be polymers or monomers that polymerize later in the reaction medium. In many cases, polymers used in the preparation of polymeric NPs are not soluble in water which requires having an organic solvent to dissolve them and the active principles. Afterwards,

emulsions are formed, and organic solvents are removed either by solvent dilution, evaporation, or salting-out. Nonetheless, not all methods require the preparation of emulsions, as in the nanoprecipitation method, where the organic phase carrying polymers is added to the aqueous phase, the hydrophobic forces of the polymer added to water are enough for particle formation (33,35,36).

Polymeric micelles are mostly circular nanostructures of 10 - 200 nm. They result from the self-assembly of amphiphilic copolymers giving rise to a hydrophobic core and a hydrophilic shell that imparts stability to the system and incorporates water-insoluble drug molecules (37). PEG is the best example of shell-forming polymers, as besides its hydrophilicity, it helps the particles escape the immune system increasing, therefore, drugs' circulation half-life. Polysaccharides, such as carboxymethyl chitosan, are also used as the hydrophilic part of those amphiphilic copolymers. As for the hydrophobic part, polylactic acid (PLA), a FDA-approved polymer, is commonly used (37,38). Those systems are very important to overcome the hurdles of drug solubility when providing targeted delivery. Micelles are widely studied for the delivery of cancer therapy basically due to the decreased solubility of those drugs. Genexol<sup>®</sup>-PM is a copolymer micelle loaded with paclitaxel, which is marketed in South Korea, and in Bulgaria and Hungary in Europe for the treatment of metastatic breast cancer (37). Depending on their size, charge, composition, and functionalisation, those systems can overcome several biological barriers in the body, improving drug targeting (38). For example, the micellar formulation CEQUA<sup>™</sup>, approved by the FDA in 2018 for ocular delivery of cyclosporine for the treatment of keratoconjunctivitis sicca, could overcome the problem of cyclosporin solubility reflecting in improvements in patient adherence (39–41). Micelles stand out from other nanocarriers for their easy preparation and scale-up properties. However, they have reduced stability and complex characterisation (19,39). Sometimes, drugs can be conjugated to the polymer by a covalent bond. In addition, micelles have promising applications as antimicrobials since polymers with antimicrobial properties can be used for their production, helping, thus, in limiting the current antimicrobial resistance crisis (42,43).

Dendrimers are highly branched spherical PNP characterized by extremely small dimensions (1 - 5 nm). Dendrimers' properties depend on their branching degree, as more branches mean the possibility of a higher degree of functionalisation (31,34). Like in polymeric micelles, drugs can either be encapsulated inside the dendrimer or covalently bond to it to form dendrimer prodrugs. Dendrimers can deliver drugs to specific cells in the body and are able to attach antibodies or aptamers, which renders them very important in cancer therapies (44).

## Polyelectrolyte Complexes from chitosan and carrageenan: optimization by Response Surface Methodology and method validation

Within the domain of antimicrobials, VivaGel® (SPL7013 Gel, astodimer sodium), a vaginal microbiocidal, is an example of a commercialised dendrimer-based formulation that showed efficacy against human immunodeficiency virus (HIV) and herpes simplex virus (HSV). This astodimer is also used in the prevention and treatment of bacterial vaginosis. More research and trials are ongoing to generate further dendrimer-based formulations; an example to highlight is the intravenous dendrimer-based docetaxel which is in phase II clinical trials for an application in the treatment of solid tumours. According to the results of those trials, the dendrimer-docetaxel showed a significant reduction in docetaxel's toxicity (45–47).

Polymersomes are nanovesicles whose structure is quite similar to liposomes but result from the self-assembly of high molecular weight synthetic amphiphilic block copolymers instead of phospholipids. Despite being very similar to liposomes, polymersomes have a thicker membrane (3 - 4 nm) and higher plasma half-life (48). Their hydrophobic chains' entanglements attribute higher stability and more drug "retention". Moreover, it is easy to increase polymersomes' circulation time by using block copolymers with PEG. Despite their versatility, they are very limited in clinical trials. That, in fact, can be connected with the reduced number of FDA-approved synthetic polymers and the high number of approved phospholipids (37,46,48).

Polymer-lipid hybrids are considered a combination of polymer and lipid NPs. Those NPs can overcome the limitations of both liposomes, such as storage instability, restricted surface modifications, and high production costs, and polymeric NPs, like limited drug-loading capacity, upscaling difficulties, and reduced plasma half-life. In general terms, polymer-lipid hybrids are composed of three layers: polymeric, lipidic, and PEG from the core to the shell (49).

Polyplexes and polymer-drug/proteins conjugates will be discussed in the section 1.3 addressing polyelectrolyte complexes.

## 1.2 Polyelectrolytes

Polymers are remarkably the most common materials used in the construction of nanotechnology-based drug carriers, as according to their nature, the customisation of many properties like hydrophobicity, molecular weight, and biodegradability is possible (21).

Polyelectrolytes (PEs) or polyions combine polymers and ions in one molecule. Polyions are very ancient molecules, given that life entails the replication of charged polymers to pass genetic information in the form of RNA (**Figure 1.5**) or DNA. Interestingly, PEs might have formed even before the beginning of life (50).

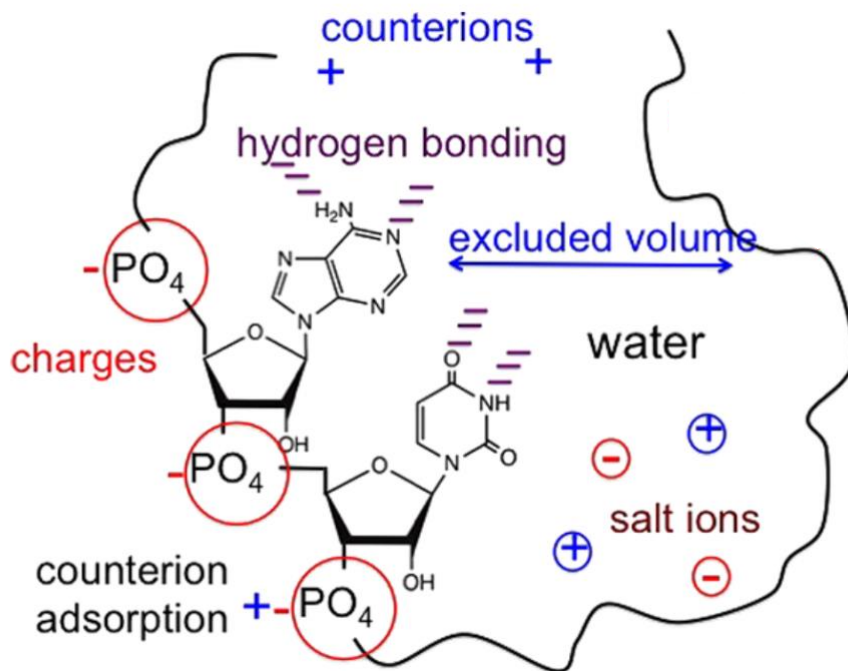


Figure 1.5 - The structure of RNA, a polyanion. Adapted from (50).

A PE is defined as any macromolecule consisting of repeating units that dissociate into a charged polymeric molecule when placed in ionizing solvents such as water leading to the formation of polyanions or polycations. PEs are always found associated to small counter-ions that lead to neutrality (**Figure 1.5**); positive counter-ions in the case of polyanions and negative in the case of polycation (51,52).

PEs, either synthetic or natural, have wide applications in nanotechnology, particularly if they evidence biocompatibility and biodegradability. Some examples of synthetic PEs

commonly used in drug delivery are poly(acrylic acid), poly(L-malic acid), and poly(methacrylic acid). Examples of natural ones are carboxymethylcellulose, alginate, heparin, chondroitin, chitosan, and carrageenan. The last two were used in this work and, thus, are further discussed in the next sections (10,53–55).

### 1.2.1 Chitosan

Chitosan (CS) is a positively charged pseudo-natural polysaccharide that owns many applications in pharmacy and biomedicine. It is the most important chitin-derived PE. It results from the deacetylation of chitin either by using deacetylases or under alkaline conditions. Chitin is the second most important natural polymer in the world after cellulose. It is found in several marine creatures but is mainly extracted from shrimp and crabs, since it is found in their exoskeleton. It is also found in the cell walls of yeast and fungi imparting strength to their structures. After acidic extraction followed by alkaline extraction, chitin is exhaustively purified from any left proteins or pigment contaminants. Naturally, chitin shows decreased solubility in many classic solvents. However, some protocols instruct that dissolving chitin at low temperatures with NaOH results in amorphous chitin with higher water solubility. Solubility can be attributed to the resulting high deacetylation (50% deacetylation provided that acetyl groups are regularly dispersed) and decreased molecular weight under drastic alkaline conditions (55–57).

CS is composed of *N*-acetyl-D-glucosamine and D-glucosamine units (58,59). CS turns into a PE in acidic media after the protonation of the primary amino groups on glucosamine units (**Figure 1.6**). It is obtained by deacetylation of chitin to an extent higher than 50% and is characterized by its solubility in acidic solutions (57). Nevertheless, the most popular degree of deacetylation of commercial CS varies within 75 - 80% (60).

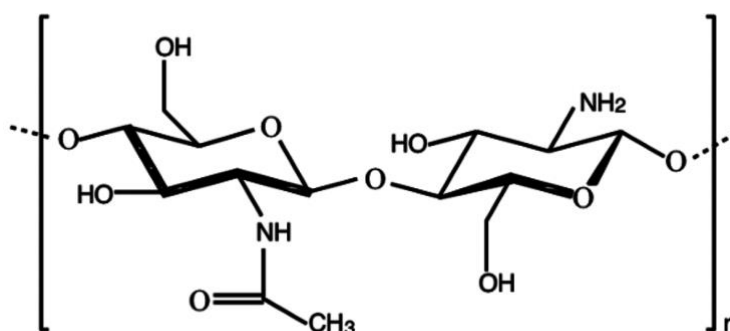


Figure 1.6 - The chemical structure of CS, composed of D-glucosamine (right) and *N*-acetyl-D-glucosamine (left) units. Adapted from (59).

Absence of toxicity, biocompatibility, biodegradability, and biological activity are frequently reported and render CS a great candidate for many biomedical applications (57,58). CS applications depend on its versatile properties which vary according to the degree of deacetylation, the distribution of the acetyl groups, and the molecular weight (57). For example, it was shown that decreasing the deacetylation degree from 100 to 40% lead to a 1.4-fold increase in the polymer stiffness. However, further decrease did not influence the stiffness of the polymer (61). It also depends on the pH, ionic strength, and how the solvent is acidified. Furthermore, the protocol followed to derive CS from chitin can also influence the properties of the former (57).

Owing to all the aforementioned properties, CS has ever had medical applications, as before the drug delivery revolution witnessed nowadays, it has been used in wound healing, and weight loss regimens (58). Furthermore, owing to its positive charge obtained in acidic solutions (21), it is very mucoadhesive, as electrostatic interactions form with the negatively charged glycosaminoglycans on cell surfaces, which, in turn, increases drug residence time on the targeted site. Positive charge also grants CS high interaction potential with a wide range of molecules, thus, versatility in the field of drug delivery (62,63). For example, CS-based NPs are proposed to encapsulate a wide range of molecules, including anti-cancer drugs, RNAs, DNAs, and proteins. This means they have high potential in gene therapy and as vaccine carriers, mainly because several studies reported no structural alterations in proteins after encapsulation in CS-based NPs (57,58,64). In addition, CS can play a role as adjuvant in vaccination, which makes it a good candidate as an excipient in vaccines delivery (55). Regarding cancer therapy, CS is also easily conjugated to other molecules such as folate, an important ligand of cancer cells (10,65), and glucose, that is captured excessively by tumoral cells (66) enabling, thus, targeted therapies.

Finally, despite all the promises built on CS formulations, its application is challenging due to its reduced solubility at physiological pH. This might explain the very few CS-based pharmaceutical products available on the market (55).

### 1.2.2 Carrageenan

Carrageenans (CRGs) are naturally occurring polysaccharides, being extracted from red algae (Rhodophyta), corresponding to sulphated esters of polygalactose of high molecular weight.  $\beta$ -carrageen is an exception, since it is deprived of sulphate ester moieties (67). Depending on the degree of sulphation and the positions of the sulphate groups, CRGs are

classified into 5 main groups:  $\lambda$ ,  $\kappa$ ,  $\iota$ ,  $\epsilon$ ,  $\mu$ . In general, sulphation degree varies from 22% to 35%. Interestingly, CRGs can be transformed from one to another by chemical modifications.  $\kappa$ -CRG, the most commonly used, is composed of alternating units of 1,3-linked  $\beta$ -D-galactose, where a sulphate group is bond to C4, and 1,4 linked anhydrogalactose units (68,69), as shown in **Figure 1.7**.

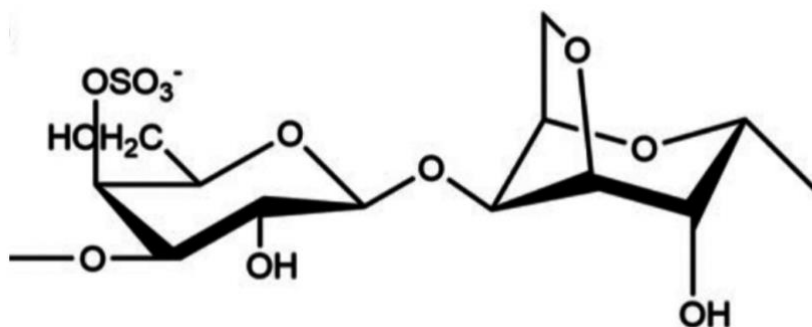


Figure 1.7 - The structure of  $\kappa$ -CRG composed of 1,3  $\beta$ -D-galactose (left) 1,4 anhydrogalactose (right) units. Adapted from (68).

Owing to their rheological properties, CRGs have wide applications in the food and pharmaceutical industries as thickeners and stabilizers (68,70). CRGs have been used since 1905 in food preparation owing to their gelling properties (68), and have been on the market as food additives since 1937 (71).

CRGs are soluble in hot water, but the temperature at which they dissolve decreases with the degree of sulphation; for instance,  $\lambda$ -CRG that has three  $\text{SO}_3^-$  groups is soluble in cold water, meanwhile  $\kappa$ -CRG with only one  $\text{SO}_3^-$  is soluble only in hot water. In addition, CRGs are soluble at high pH (68,72).

CRGs own different biological activities, for instance, they can function as anticoagulants. Studies have shown that the most potent CRG possesses 1/15 of heparin's activity. Surprisingly, it has the same mechanism of action as heparin as both act on thrombin inhibition. CRG's anticoagulant activity is slightly dependent on Antithrombin-III, but they inhibit the amidolytic activity of thrombin as well (73–75). Moreover, CRGs have antiviral activities against many viruses such as HSV and human papilloma virus (HPV) (73). Studies have proven that  $\iota$ -CRG is effective against a strain of influenza virus, and its effect is similar to the one of oseltamivir (73,76). They can also have anti-cancer, anti-metastatic, and anti-

oxidant activity as they eliminate free radicals and stimulate the immune system; they also have cholesterol-lowering properties (73).

Regarding drug delivery, CRGs have been used in many domains, namely in nanotechnology. For example,  $\kappa$ -CRG is used in the preparation of thermosensitive nanogels; gels that increase in volume with temperature increase (77). Other studies showed the potential of CRGs in encapsulating insulin in microparticles for oral delivery and found that CRGs confer protection from drastic gastric conditions (78). Interestingly, CRG/CS nano- and microparticles were also found to confer stability and protection to proteins encapsulated for nasal and pulmonary delivery (79).

Despite being approved by regulatory agencies as a food additive and in pharmaceuticals as an excipient in tablet manufacturing, CRGs are still not considered completely safe (70,71), as some concerns still arise around them. For example, it is not legislated for an application in infant formulas in Europe, yet, since some inflammatory side effects can appear upon its application. Interestingly,  $\kappa$ -GRG, the one used in our study, was found to be the least pro-inflammatory one (69,80,81). Owing to those secondary effects, CRGs are used to induce oedema in lab rats to test anti-inflammatory drugs (73). The harmful effects of CRGs are attributed to small molecular weight derivatives, mainly poligeenan, or to final bacterial degradation products such as sulphide (69).

### 1.3 Polyelectrolyte complexes (PECs)

The history of polyelectrolyte complexes (PECs) goes back to 1896 when a scientist unravelled phase separation and the role of electrostatic interactions in the complexation of two natural PEs of proteins and carbohydrates. Afterwards, in 1930, natural complex coacervates were defined underlining the importance of PECs. However, more thorough research on PECs was done in 1961 by studying the stoichiometric complexes formed from two synthetic polymers. Only after 1961, PECs became a point of attraction in research and development (82). Some examples of naturally occurring PECs are nucleosomes, the building units of chromosomes, as electrostatic interactions happen between DNA (negative PE) and histones (positive PE) (51).

Benefits are taken from DNA's negative charge in applications of gene therapy, resulting in polyplexes that are considered promising carriers for gene delivery. Polyplexes (**Figure 1.4**) result from the complexation between nucleic acids and polycations, and their importance comes fundamentally from being a safer alternative to viral carriers (21,56,83). Studies showed

CS as a good candidate for the formation of polyplexes since polyplexes of less than 100 nm could be obtained (56,84,85).

Besides polyplexes, PECs are the base of smart delivery systems, mainly on the nanoscale. Studies investigated the importance of PECs in protein delivery to protect proteins and increase their stability in the first place. For example, a comparative study has shown that PECs of the two natural PEs, CS/CRG, are highly stable and confer protection to glucose oxidase, potentiating its delivery. Among the tested CRGs,  $\kappa$ -CRG provided the highest protection and the slowest release of the protein (86). Moreover, PECs from two synthetic PEs, poly(acrylic acid)/ poly(allylamine hydrochloride) were found to confer protection to bovine serum albumin, a protein model, in their complex coacervate (87).

Drug delivery strategies based on drug carriers are promising in addressing antimicrobial resistance. PECs are not less important than any other drug carriers in antimicrobials delivery since they have shown great potential in encapsulating antibiotics and overpass hurdles related to their bioavailability and targeting. A study reported designing vancomycin (a glycopeptide antibiotic)/ poly(acrylic acid) polyplexes, drug/PE complexes (**Figure 1.4**), that would serve as promising pulmonary delivery system (88). Moreover, ciprofloxacin is a poorly water-soluble antibiotic that can form nanoplexes with oppositely charged polymers such as dextran sulphate, leading to the formation of amorphous PECs, therefore higher dissolution rate and bioavailability of the antibiotic (89).

Nanoplexes were studied and developed for other medical ends. For instance, nanoplexes mimicking viral envelopes were generated to overcome biological barriers as mucus penetration and enzymatic susceptibility in insulin delivery. Particles were prepared by complexing CS-phenylalanine copolymers with insulin and later coating them with sodium dodecyl sulphate – a surfactant. *In vitro* studies have shown that those nanoplexes improved the oral delivery of insulin especially when coated with the surfactant (90).

### 1.3.1 Characterisation of PECs

Many techniques are employed to characterise PECs, that is, investigate their physicochemical properties, such as size, zeta potential, shape, and surface characteristics. The most importantly applied ones are detailed below.

#### 1.3.1.1 Zeta potential

Zeta potential (ZP) of a particle in dispersion is defined as the difference in potential between the fluid where the particle is dispersed and the fluid layer where the counterions of

the particles are found (91). ZP is very important in the characterisation of PECs (92) since it measures the surface charge, which has a reflect on colloidal stability *ex vivo*, *in vivo*, and its shelf-life, especially since the high ionic strength of *in vivo* fluids can lead to the aggregation of those particles which, in turn, has devastating consequences (91,92). ZP is also an important tool to assess particles' affinity for cell surfaces, given that the latter are negatively charged due to glycosaminoglycan groups (62,93).

High values of ZP indicate dispersion stability because enough repulsion is there to avoid flocculation events facilitated by Brownian motion, that moves particles closer to each other and boosts interactions. In general, dispersions with  $ZP > |30|$  are considered stable (7,94–97).

Many factors can influence ZP values. Those can be either related to particles' features like size and concentration, or related to solvent properties like conductivity, pH, and temperature (94). In general, NPs or PECs tend to coagulate and agglomerate favouring the reduction of their surface energy. However, stable systems are obtained either by electrostatic or steric repulsion achieved by relying on polymers or surfactants. In addition, increased PECs concentration in the medium leads to lower stability due to higher chances of collision, thus, of agglomeration (91,96).

Electric double layer theory (**Figure 1.8**) is generally used to explain the NP-dispersant interaction. This theory states that every dispersed NP is surrounded by two layers of ions; the inner one is called Stern layer and has oppositely charged ions. Stern layer is inherently bound to the particle. The outer layer is called the diffuse layer and is more loosely bound to the particle. Slipping plane is an imaginary boundary within the diffuse layer; ions within the slipping plane move along with the particle in dispersion while ions outside this boundary stay in place. The potential difference between the particle's surface and the dispersing liquid on the slipping plane is called ZP (97,98).

ZP is measured using electrophoretic light scattering (ELS). Voltage application on a cell where PECs are dispersed leads to particles' movement. Later, a laser beam is forwarded to this dispersion. The intensity of the scattered laser light fluctuates at a frequency proportional to the particle velocity upon voltage application (91).

Besides ELS, other less common methods are used to detect the stability of nanodispersed systems, such as ultraviolet-visible (UV-Vis) spectroscopy and transmission electron microscopy (TEM) considering their ability to detect agglomeration (91).

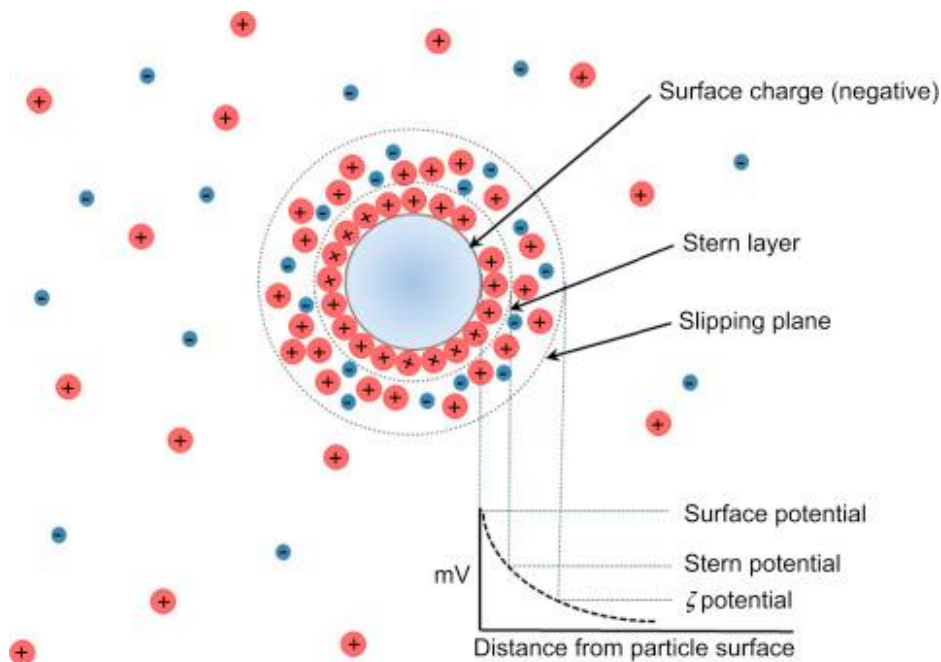


Figure 1.8 - Electric double layer. Adapted from (97).

### 1.3.1.2 Size

The size of PECs is very critical for their characterisation since it indicates how small those therapeutic materials are in comparison to the different body compartments (**Figure 1.1**). For instance, the size of the smallest capillaries in the human body is 4  $\mu\text{m}$  in diameter, thus therapeutic PECs size cannot surpass this value (6).

The characterisation of particles' size is based on light scattering phenomena. These phenomena were first described by John Tyndall, that studied light scattering from colloidal suspensions; this is known as Tyndall effect and happens when particles are larger than the wavelength of the incident light (99). Particles' size and shape are characterized by dynamic light scattering (DLS), scanning or transmission electron microscopy (SEM, TEM), or by atomic force microscopy (AFM). Given that DLS is the most common one and that it was used in this study, it will be discussed in detail (6).

DLS can measure particles of 0.3 nm to 10  $\mu\text{m}$ . This technique is based on the interference of a light beam with dispersed particles experiencing Brownian motion. The size of NPs is correlated to their velocity (Diffusion Coefficient; determined by Stokes-Einstein equation (**Equation 1**)) (6). DLS also provides the values of size distribution as an index called Polydispersity Index (PDI) that ranges from 0 to 1, where 0 is obtained in very homogenous dispersions and 1 is obtained in very heterogenous ones (96). Measuring particles' size depends

on analysing light intensity alterations as a function of time. When a laser beam passes through a dispersion containing PECs, its intensity will change. Bearing in mind that smaller particles diffuse faster than larger ones, instruments measure size correlated particle size and time-dependent light scattering capacity. DLS, in addition to providing size measurements, gives an indication of colloid stability once it can detect the presence of agglomerations especially since the PDI increases with the increase of agglomeration. By employing the Stokes-Einstein equation (**Equation 1**), instruments are capable of identifying the size (6).

$$D = \frac{kT}{6\pi\eta Rh} \quad (1)$$

Where D is diffusion coefficient, k is Boltzmann's constant, T is temperature,  $\eta$  is solvent viscosity, and Rh is the rheodynamic radius of particle solution

The advantage of DLS over the other methods is that it gives more representative measurements once it provides the average measurement of the whole sample, meanwhile AFM or TEM provide information about a small portion of the sample (picture of NPs). Moreover, DLS is highly important due to its versatile applicability as it can be used in physiological fluids, at different temperatures and pH values. In addition, this technique is fast and simple (100). However, it is important to adjust the concentration of particles measured by DLS since besides size, this technique depends on the concentration of the analysed particles (99,100).

### 1.3.2 Mechanisms of formation of PECs

In order to understand the factors that influence PECs formation and properties, it is essential to primarily comprehend the mechanisms underlying their formation. Those mechanisms are discussed in this section, and they depend on variables related to the PEs themselves and to the surrounding conditions.

As aforementioned, PECs result mainly from the electrostatic interactions between two oppositely charged PEs. In a suitable polar environment, normally water, the complexation between polyanions and polycations leads to PECs formation. Those PECs separate later into two phases: diluted and concentrated ones. The concentrated phase can be either a coacervate, a precipitate, or a gel. Moreover, PECs can remain soluble (82). Therefore, polyelectrolyte complexation can result in the following three types of PECs (62,82):

- Soluble: result from the non-stoichiometric interaction between two PEs bearing weak charges, and large differences in molecular weight (**Figure 1.9**) (101).

- Colloidal: also result from non-stoichiometric mixing in a very diluted solution of PEs bearing low to medium charge, and they are characterized by Tyndall effect.
- Two-phase PECs: PECs precipitate out of the solution. Aggregation of PECs takes place when there is a charge ratio of 1 between both PEs (56). In this category, the interacting polymers have both high molecular weight and are found at high concentrations. In addition, studies have shown that at this point of charge neutralisation, increase in particle size and distribution is reported (101,102).

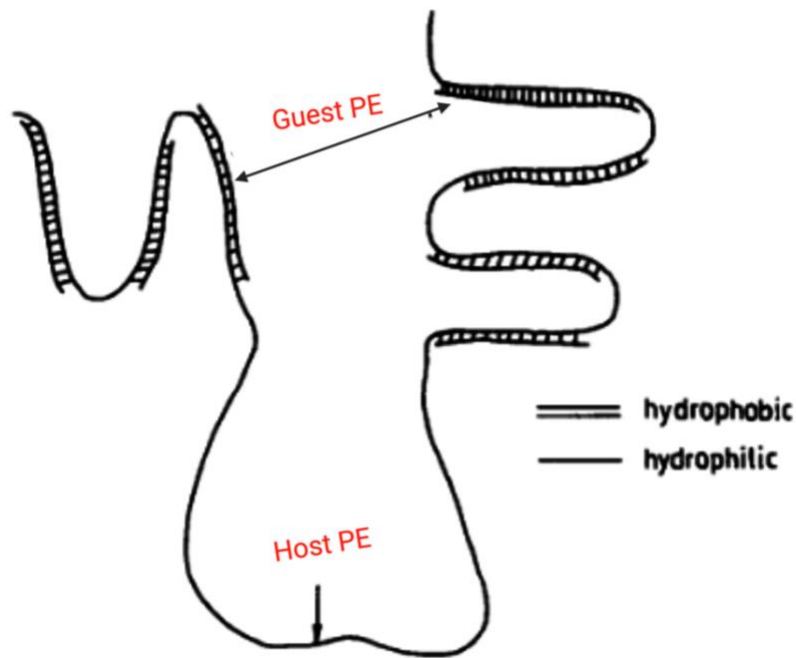


Figure 1.9 - The formation of soluble PECs: there is a large host PE and a small guest PE. Adapted from (101).

Some authors proposed the core-shell model to interpret the formation of PECs (103,104) from alginate/CS, and dextran sulphate/CS, respectively. This model implies the presence of a host PE, the PE in excess, and a titrated PE, the one added to the host. After the addition of the titrated PE, a hydrophobic core and a hydrophilic shell is formed with a charge like the one of the PE in excess. The PE in excess is responsible for stabilizing the PEC (103). When the PE in excess is smaller than the one added to it, the resulting PEC depends on its neutralisation capacity. Also, according to this model, the aggregation results from the neutralisation taking place between oppositely charged small patches of PECs (103,104).

There are also two structural models discussed in the literature and depend on the characteristics of the polyion groups, relative rearrangement, stoichiometry, stereoregularity and molecular weight. Those two models are explained below:

- Ladder model (**Figure 1.10-a**) suggests the presence of single and double strands of PEs, where the first are hydrophilic and the last are hydrophobic. According to this model, PECs are normally formed when PEs that have weak ionic groups and a big difference in molecular dimensions are mixed (see the part about soluble PECs) leading to the formation of soluble as well as insoluble PECs; sometimes, PEs with high molecular weight and weak charge density are added to short PEs (smaller molecular weight) with opposite charge, so-called oligomers, forming initially soluble PECs and later with continuous addition, insoluble PECs (105). The ladder structure results from the so-called “zippering action” as one reaction leads to the reaction of the site immediately nearby (106).
- Scrambled egg model (**Figure 1.10-b**) is normally used to describe the interaction between two PEs when some charges on one of the PEs are not accessible to interact with the opposite charges on the other. This can happen due to many reasons such as steric hindrance, lack of PEs flexibility, or even due to charge distribution (103). Those PECs normally result from the interaction between PEs with strong ionic groups and similar molar masses, leading to the aggregations in the case of stoichiometric complexes; stoichiometry of 1:1 (105,106).

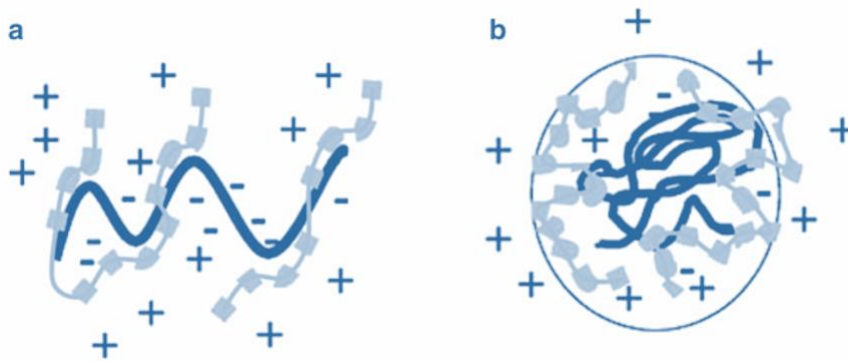


Figure 1.10 - Ladder (a) and scrambled egg (b) structures of PECs. Adapted from (107).

The formation of PECs can be enthalpy- or entropy-driven and is inherently related to salts concentration in the reaction medium (**Figure 1.11**). When two oppositely charged PEs react and form PECs, they release their counterions, which, in turn, leads to changes in the enthalpy (energy) and entropy of the system. PECs formation can be entropy-driven; entropy increases due to the released counterions into the solution, thereby, in high ionic strength solution (solutions with high salts concentration) the entropy gain resulting from counterion

release is less as salts hinder entropy driven PECs formation. Despite the loss of configurational and translational entropy of PEs verified upon complex formation, which opposes complex formation, in polymers with long chains this loss is smaller compared to counterion entropy gain, and the result is entropically favoured reactions. Also, according to salts concentration, complexation can be endo or exothermic. It is exothermic at low salt concentrations and endothermic at high salt concentrations (**Figure 1.11**). In the case of weakly charged PEs, the reaction is exothermic, but for strongly charged chains, it is endothermic because there is a large portion of counteractions strongly bound to PEs before complexation. Other interactions in the formation of PECs can take place such as hydrogen bonds or hydrophobic interactions (51,108–111).

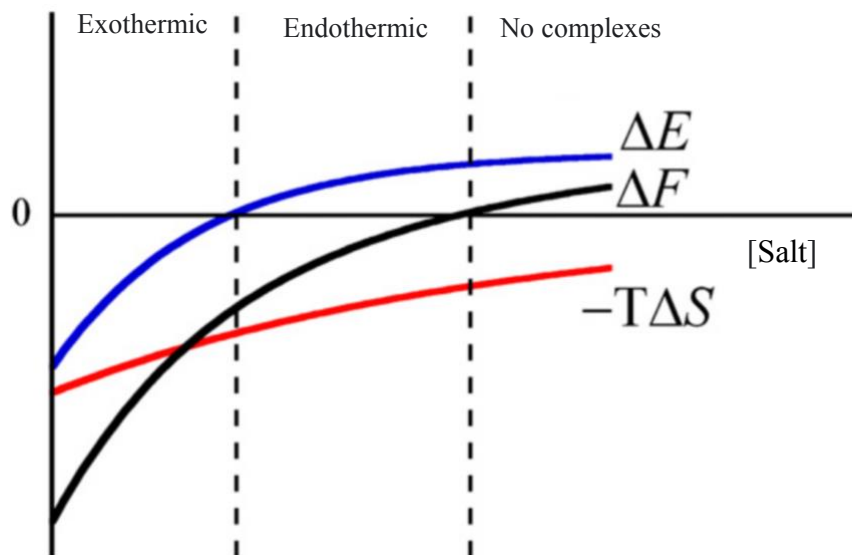


Figure 1.11 - PECs formation can be endothermic or exothermic according to salt concentration.  $\Delta F$ : the total free energy of the complexation reaction,  $-T \Delta S$ : counterion release entropy,  $\Delta E$ : Coulomb energy. Adapted from (51).

### 1.3.3 Factors that affect PECs formation

There is a set of factors that influence the formation of PECs, as shown in **Figure 1.12**. Some are related to PEs themselves such as charge density and molecular weight, while others are related to the solvent such as temperature, ionic strength, type of salt, solvent polarity, and pH (82,109,111,112). In the following sections, the effects of pH and ionic strength of the solvent will be discussed.

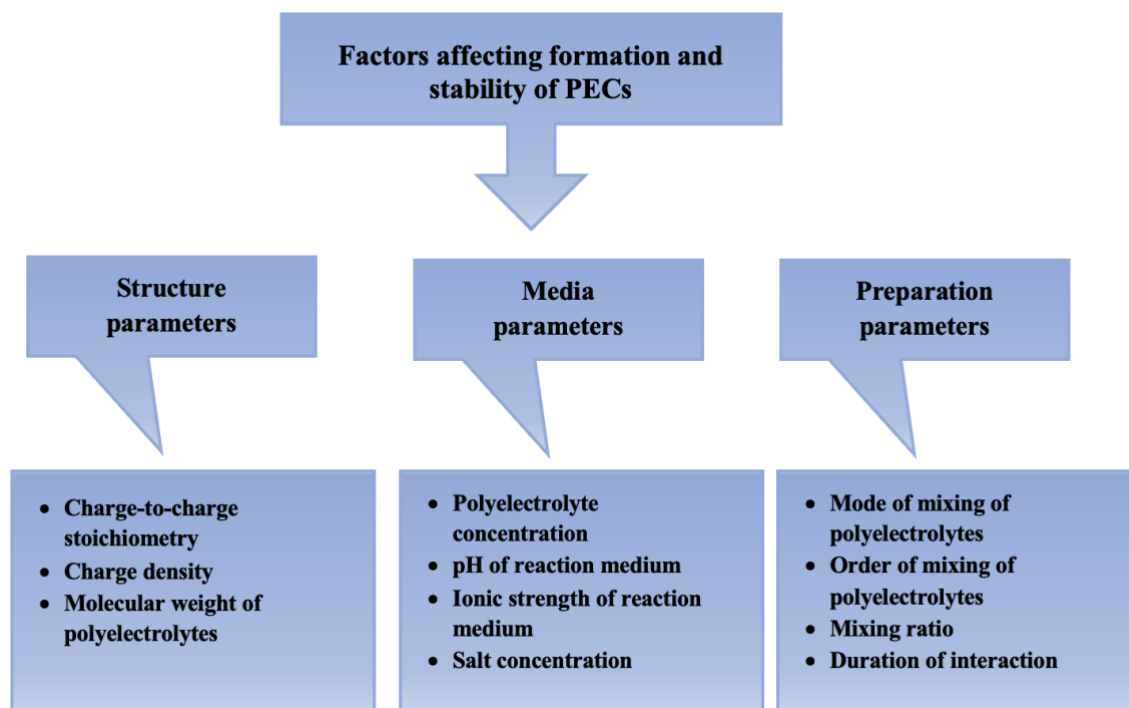


Figure 1.12 - Factors that influence PECs formation. Adapted from (112).

### 1.3.3.1 pH effect

The pH of PECs is an important feature to be studied and analysed since it influences many properties of these complexes such as size and ZP, thus, affecting the stability (112). This effect comes from its influence on the dissociation of polyacids and polybases. Having that said, it is particularly important in the case of weak acids and bases since strong ones are always found dissociated (52). Changes in the pH of the medium of weak acids/bases causes alterations in the number and distribution of ionised groups, thus, of the ones available to interact. Furthermore, pH can lead to changes in the conformation of PECs resulting, sometimes, in less exposure of functional groups or formation of secondary structures and less interactions (105,111,113–115).

In fact, PECs are not influenced only by the pH of the reaction medium, but also of the different body compartments, leading, therefore, to different release profiles of encapsulated drugs. **Figure 1.13** below shows that PECs obtained from CS and heparin swell at acidic pH and aggregate at basic pH, altering, consequently, the release profile of the encapsulated drug. (112,115). Furthermore, pH can influence the cellular uptake of CS-based PECs due to the less protonated CS in high pH (116).

Polyelectrolyte Complexes from chitosan and carrageenan: optimization by Response Surface Methodology and method validation

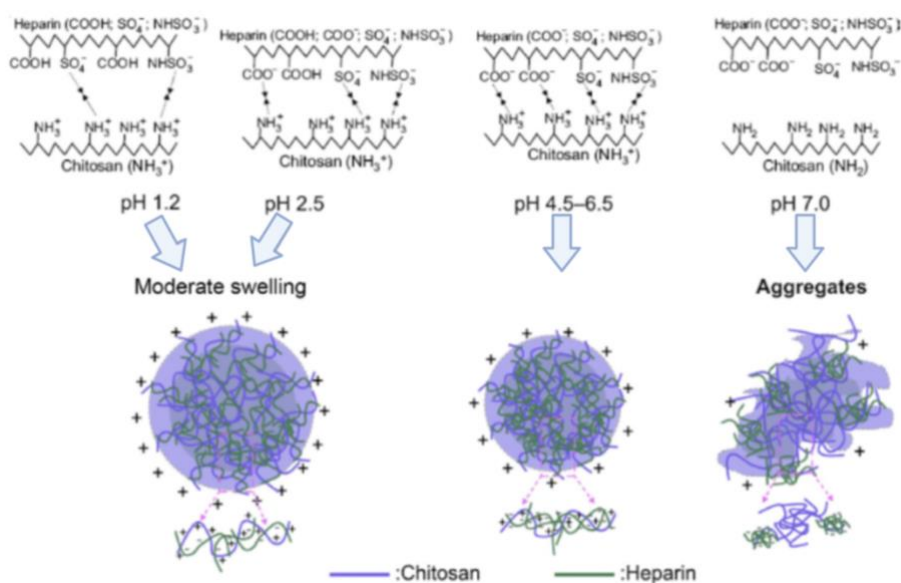


Figure 1.13 - The effect of pH on PECs from CS and heparin. Adapted from (115).

### 1.3.3.2 Ionic strength effect

As mentioned in previous sections, PECs are very sensitive to the ionic strength of the solvent. When the concentration of a salt in the surrounding media is increased, it leads to increased PE-salt interaction and decreased PE-PE electrostatic interactions (56).

High concentrations of salt influence the release of counterion as it decreases the entropy-driven force to do so, leading to decreased PECs formation. However, low salt concentration might have a beneficial effect on PECs formation. A study (113) found that adding a small amount of salt ( $< 75$  mM) enhanced complex formation (turbidity measurements revealed an increase in size and number). Low concentrations of salt improve complex formation by improving the conformation and flexibility of PEs chains making them more accessible to react (113,114), and also by reducing inter and intra-molecular repulsion (89). **Figure 1.14** represents the interaction between a PE and ciprofloxacin and highlights the importance of salt in the formation of nanoplexes. Moreover, it was found out that the increased flexibility resulting from high ionic strength leads to the formation of smaller PECs. However, further addition of salt leads to null turbidity due to complex dissolution (113,114). Another study found that PECs tend to aggregate in the presence of NaCl (91). In addition to the aforementioned study (114), another one found that the size of PECs increased upon the addition of  $\text{Cl}^-$  salts until 0.5 M of salt concentration, decreasing for higher concentrations (117).

Interestingly, divalent salts were found to have lower critical salt concentration, which is the concentration of salt at which it stops enhancing complex formation, than monovalent ones,

## Polyelectrolyte Complexes from chitosan and carrageenan: optimization by Response Surface Methodology and method validation

and cations had a stronger effect than anions. Chaotropic ions such as  $\text{Ca}^{2+}$  and  $\text{I}^-$  are known for their salting-in effect as they increase polymers' solubility (113). In conclusion, salt concentration can influence the size of PECs, either increasing or decreasing according to the salt and its concentration.

It is noteworthy that the same charge over one polymer chain leads to intrinsic repulsion, therefore an extended polymer. Extended structures were verified at low salt concentrations of the solvent. When this ionic strength is increased, the solution becomes thicker (52). Repulsion is also influenced by friction charges over the polymer chain, as the lower the friction charge the more extended the polymer chain (82).

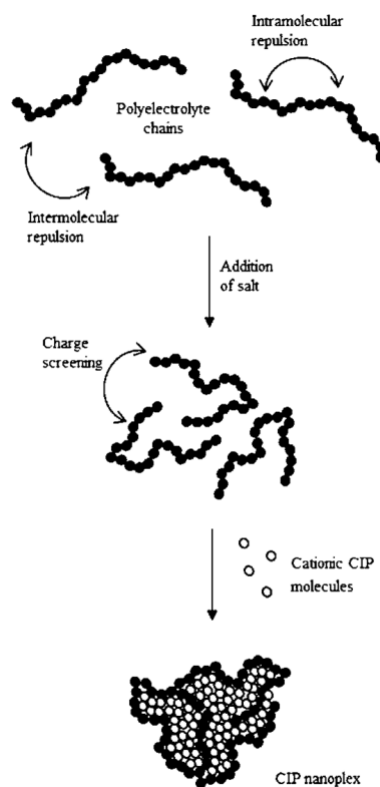


Figure 1.14 - The effect of NaCl on the formation of nanoplexes from ciprofloxacin (CIP) and a PE. Adapted from (89).

Studying the effect of salts on PECs is very important, mainly in pharmaceutical applications, as the effect of corporal salts on medically employed PECs cannot be underestimated and can influence their size and/or stability. Finally, adding salts to PECs in precipitation makes the formation of liquid coacervates easier. However, at the critical salt

concentration, that is, adding excessive amounts of salt, prevents the formation of any PEC (56,113).

## 1.4 Response surface methodology (RSM)

Response surface methodology (RSM) is an old methodology. Its development goes back to the 1950s. Nowadays, that old methodology is called the classical RSM (118). As the name suggests, RSM is a group of statistical and mathematical methods used to find a relationship between a group of independent variables and a response (dependent variable). This response is a surface obtained after fitting a mathematical model. The use of this methodology requires an adequate experimental design (118,119).

It is important to shed the light on two different terms which are the experimental domain and experimental design. The first results from the points obtained experimentally and the second from the points predicted by the design by making different combinations between the independent variables to obtain the dependent ones (119). Usually, designs are constructed to find a function ( $f$ ) that binds between dependent and independent variables. However, finding the real function is challenging in many cases, therefore, functions estimation, finding a function that best reflects the real one, is the main responsibility of the experimenter (120).

Initially, the most commonly chosen functions are the first order (**Equation 2**) or second order polynomial functions (**Equation 3**) (120):

$$\eta = \beta_0 + \beta_1 x_1 + \beta_2 x_2 + \dots + \beta_k x_k \quad (2)$$

$$\eta = \beta_0 + \sum_{j=1}^k \beta_j x_j + \sum_{j=1}^k \beta_{jj} x_j^2 + \sum \sum_{i<j=2}^k \beta_{ij} x_i x_j \quad (3)$$

Where,  $\beta$ s are unknown coefficients and can be estimated based on the experimental data. The estimation of the regression coefficients  $\beta$  is called model fit and is normally done using the method of minimal squares (120).

RSM has many applications in science, engineering, and industry such as in microbial cultures to optimize products fermentation (121), vehicle designing (122), and the food industry (123). Furthermore, RSM has a good contribution to the world of drug delivery, such as the preparation of nanoemulsions (124) microspheres (125) microparticles (126), and hydrogels (127), among others.

RSM is used with different goals such as: constructing the response surface over a region of interest for future predictions of the consequences resulting from varying the experimental conditions (predicting size variations of PECs with the variation of CRG concentration is an

example from the current study), and optimizing the experimental conditions to obtain the desired response (120). An example from this study is defining the ideal concentrations of CRG, CS, and salt to obtain the smallest PECs possible.

In mixture experiments, the factors of the experimental design are components of a mixture, and the response is a function of the proportions of the ingredients. Also, in this type of experiments, the levels of those factors are interdependent, that is, in an experiment with  $p$  factors (components), the following must be satisfied: (120)

$$\sum x_i = 1 \text{ where } 0 \leq x_i \leq 1 \quad (4)$$

The most commonly used mathematical models used in mixture experiments are (120,128):

$$\text{Linear: } E(y) = \sum_{i=1}^p B_i x_i \quad (5)$$

$$\text{Quadratic: } E(y) = \sum_{i=1}^p B_i x_i + \sum \sum_{i < j} B_{ij} x_i x_j \quad (6)$$

This type of experiments is found to have applications in diverse areas, such as formulations where products are obtained by mixing different ingredients together; in the case of the chemicals and foods industry (120).

## 2 Objectives

This project is part of a wider research project related with the optimisation of the formation of PECs on the nanoscale. In this research we focused on optimizing the formation of PECs from two oppositely charged polysaccharides, CS and CRG, in the presence of NaCl. An experimental design was built using the RSM and this method was further validated.

### 3 Materials and methods

#### 3.1 Materials

Chitosan (CS) of low molecular weight (deacetylation degree = 75 - 85%, Mw = 3216 kDa Mn = 119 kDa ), sodium azide, NaCl  $\geq$  99%, granular anhydrous CaCl<sub>2</sub>  $\geq$  93.0% and Na<sub>2</sub>SO<sub>4</sub>  $\geq$  99% were purchased from Sigma Aldrich<sup>®</sup> (Germany). One  $\kappa$ -CRG (Mw = 16420 kDa, Mn = 979 kDa) was obtained from FMC BioPolymer<sup>®</sup> (Norway), while another  $\kappa$ -CRG (Mw = 29212, Mn = 1304) was obtained from Sigma Aldrich<sup>®</sup> (Germany). Glacial acetic acid was from Merck (Germany), and HCl 37% from VWR Chemicals<sup>®</sup> (France). Ultrapure water (Millipore<sup>®</sup>, Portugal) was used to prepare all the solutions. Filter paper of 3 - 15  $\mu$ m and syringe filters were purchased from VWR<sup>®</sup> (France). Dialysis tube (SnakeSkin<sup>™</sup> Dialysis Tubing, 3,500 MWCO) was supplied by Thermo Scientific<sup>®</sup> (USA).

#### 3.2 Preparation and characterisation of PECs from commercial CS and CRG

Solutions of 1 mg/mL of CS, 1.25 mg/mL of commercial  $\kappa$ -CRG from BioPolymer<sup>®</sup> (CRG *BioPolymer*) and 1.25 mg/mL of commercial  $\kappa$ -CRG from Sigma Aldrich<sup>®</sup> (CRG *Sigma*) were prepared. The CS solution was prepared in acetic acid 1% under stirring, until complete dissolution, then filtered using filter paper of 3 - 15  $\mu$ m. CRG solutions were prepared in water preheated to 60 °C. In order to guarantee the complete dissolution of CRG, solution temperature was maintained between 20 °C and 50 °C under constant stirring. After dissolution, the solution was filtered through a 0.45  $\mu$ m syringe filter.

PECs were prepared by adding 0.8 mL of each of the set CRG concentrations (1.25, 0.83, 0.625, 0.5, and 0.425 mg/mL) to 2 mL of CS (1mg/mL) under stirring for 10 min resulting in CS/CRG mass ratios of 2/1, 3/1, 4/1, 5/1, and 6/1, respectively. The process was repeated three times (n = 3) for each of the CRG sources.

PECs were characterized by measuring size and PDI using DLS, ZP using ELS by Zetasizer Nano ZS (Malvern Instruments, UK) at 25 °C.

### 3.3 Purification of PEs

Solutions of CS and CRG from FMC BioPolymer<sup>®</sup> (Norway) were prepared and dialyzed against water using a dialysis tube. For the dialysis, a solution of 5 mg/mL of each PE in distilled water was prepared and filtered. In the case of CS, HCl (2M) was added dropwise until the complete dissolution of the polymer. CRG solution was prepared as mentioned above in 3.2. Afterwards, dialyzed polymers were freeze-dried for 72h in a freeze-dryer (Labconco<sup>®</sup> FreeZone 6 Liter Benchtop Freeze Dry System freeze dryer, Labconco<sup>®</sup>, USA). The variations of temperature and pressure during freeze-drying are: (−50° C, 11.0 Pa), (−53° C, 11.0 Pa), (−51° C, 11.0 Pa), and (−50° C, 11.0 Pa) for the first, second, third and fourth day respectively. A second dialysis was performed, and the variations during freeze-drying were: (−87° C, 11.0 Pa), (−69° C, 11.0 Pa), (−80° C, 11.0 Pa) and (−83° C, 11.0 Pa).

### 3.4 Precipitation study, determining the solubility of PEs in salt solutions

To perform a preliminary study of the solubility of CS and CRG in salt solutions, solutions of purified CS (1.25 mg/ml) and CRG (1.5 mg/ml) were prepared in water at room temperature. Later, drops of HCl (6 M) were added to CS solution until complete dissolution.

Nearly saturated salt solutions were prepared in water, that is NaCl (5 M), Na<sub>2</sub>SO<sub>4</sub> (1.5 M), and CaCl<sub>2</sub> (5 M). Each salt solution was added dropwise to CRG and CS solutions mentioned above until turbidity was noticed.

### 3.5 Determining the isoelectric point (IP)

To determine the isoelectric point (IP), formulations from 1/6 to 10/1 (CRG/CS, W/W) corresponding to 0.10 to 6.10 n<sup>-</sup>/n<sup>+</sup> were prepared (**Table 3.1**). Also, formulations of 2.3/1, 2.5/1 and 2.7/1 (CRG/CS, W/W) corresponding to 1.44, 1.52, and 1.65 n<sup>-</sup>/n<sup>+</sup> were prepared trying get closer to the IP. For PECs preparation purpose, CRG was added to CS in the formulations 1/6 to 1/1 (0.10 - 0.61 n<sup>-</sup>/n<sup>+</sup>) while CS was added to the CRG in the formulations from 2/1 to 10/1 (1.20 - 6.10 n<sup>-</sup>/n<sup>+</sup>), following the procedure described above.

For the formulations 1/6 to 1/2 (0.10 - 0.307 n<sup>-</sup>/n<sup>+</sup>), CS and CRG solutions of 1 mg/mL and 1.5 mg/mL, respectively, were prepared in ultrapure water. The pH of the resulting CRG

Polyelectrolyte Complexes from chitosan and carrageenan:  
optimization by Response Surface Methodology and method validation

solution was pH = 3.54. The pH of the resulting CS solution pH = 5.4 was adjusted to pH = 2.99 by the addition of HCl (6 M). This adjustment was performed to approach the pH of CRG.

For the formulations 1/1 to 10/1 (0.61 - 6.10 n<sup>-</sup>/n<sup>+</sup>), a CS solution at 2.5 mg/mL and a CRG solution at 1mg/mL were prepared in ultrapure water. The pH of CS (initially 5.33) was adjusted to 3.38, in order to approach that of the CRG solution (pH = 3.16).

The resulting PECs were characterised by measuring size, ZP and transmittance at  $\lambda = 550$  nm. Transmittance measurements were performed in a Thermo Fisher Scientific<sup>®</sup> (Madison, USA) UV-Vis spectrophotometer.

Table 3.1 - Concentrations of CS and CRG and n<sup>-</sup>/n<sup>+</sup> ratios used to determine the isoelectric point of PECs. Formulations n<sup>-</sup>/n<sup>+</sup> = 1.80 - 4.33 precipitated (\*).

<b>CRG/CS (W/W)</b>	<b>CS mg/mL</b>	<b>CRG mg/mL</b>	<b>CS mM</b>	<b>CRG mM</b>	<b>n<sup>-</sup>/n<sup>+</sup></b>
1/6	0.71	0.12	2.854	0.294	0.10
1/5	0.71	0.142	2.854	0.348	0.12
1/4	0.71	0.177	2.854	0.434	0.15
1/3	0.71	0.23	2.854	0.564	0.20
1/2	0.71	0.357	2.854	0.875	0.307
1/1	0.71	0.71	2.854	1.740	0.61
2/1	0.36	0.71	1.447	1.740	1.20
2.3/1	0.3	0.71	1.206	1.740	1.44
2.5/1	0.284	0.71	1.142	1.740	1.52
2.7/1	0.263	0.71	1.057	1.740	1.65
3/1*	0.24	0.71	0.965	1.740	1.80
4/1*	0.18	0.71	0.724	1.740	2.40
5/1*	0.14	0.71	0.563	1.740	3.09
6/1*	0.12	0.71	0.482	1.740	3.61
7/1*	0.1	0.71	0.402	1.740	4.33
8/1	0.088	0.71	0.354	1.740	4.92
9/1	0.079	0.71	0.318	1.740	5.48
10/1	0.071	0.71	0.285	1.740	6.10

### 3.6 Construction of the Experimental Design (ED)

Maximum points of the EDs were defined basing on preliminary studies and previous studies. Four EDs were generated to obtain the one with higher prediction reliability. However, the fourth ED was elected for the construction of the response surfaces.

ED1 ( $CS_{\max} = 0.75$  mM,  $CRG_{\max} = 0.75$  mM,  $NaCl_{\max} = 0.5$  M). Those maximum values of the design are much lower than the ones obtained in the precipitation study for CS (2.22 mM of CS and 2.79 M of NaCl) and were selected to avoid any possible precipitation. It was noticed from the results of ED1 shown in **Table 7.1** that many formulations had very low Count Rate (CR) which indicates low particles concentration (111,129). Also, %T varied from 93.4% to 100.7%, except for the formulation that contains only CS where an unexpected %T = 79% was registered despite having an extremely reduced CR. ZP values were also very low in several formulations and not enough to provide good repulsion and stability even in the ones that contained the two polymers (7,94–97). Those results were enough reason to reject the ED1.

In ED2 ( $CS_{\max} = 3$  mM,  $CRG_{\max} = 3$  mM,  $NaCl_{\max} = 0.1$  M), higher concentrations of polymer (4X) and lower of NaCl (X/5) were selected, aiming to obtain higher yield by avoiding salting-out and improving the conformation of the polymer (113,114). The resulting formulations had relatively higher CR values, mainly the ones that resulted from adding all the three components. Also, lower %T values were obtained; however, precipitation took place in the formulation 7 where 1/3 of each component was added (**Table 7.2**). Consequently, a new adjustment was required for the ED2 to obtain the ED3.

In ED3 ( $CS_{\max} = 3$  mM,  $CRG_{\max} = 2.5$  mM,  $NaCl_{\max} = 0.1$  M), CRG concentration was reduced aiming to get rid of precipitation. A considerably higher CR, especially in the formulations 9 and 10, was obtained. However, precipitation was still noticed in the formulation 8 (0.167 0.167, 0.67 of CS, CRG, NaCl, respectively) (**Table 7.3**). Since no precipitation is desired, some adjustments were added to the ED3 to obtain the ED4. Point 8 was deleted and one more formulation: (0.2, 0.2, 0.60 of CS, CRG, NaCl, respectively) was prepared. The goal of this formulation was to approach the highest NaCl concentration possible since precipitation was noticed in the formulation 8 where 66.67% NaCl was incorporated.

After all, a final ED was reached, ED4, which was constructed with a minimum concentration of each of the components set at 0 and a maximum at 66.67% for CS and CRG and 60% for NaCl (**Table 7.4**). Response surfaces were obtained based on this ED.

## Polyelectrolyte Complexes from chitosan and carrageenan: optimization by Response Surface Methodology and method validation

The total number of experimental points used for the construction of the design is 15. These points were prepared as follows (**Figure 3.1**) stock solutions of CS, CRG, and NaCl were prepared and had the following concentrations: 1.38 mg/mL (6 mM), 2.04 mg/mL (5 mM), and 1.5 M, respectively. Later, mixtures of NaCl and polymer solutions were prepared for each formulation and the volume was completed to 1.5 mL with water (pH = 2.5) as shown in (**Table 7.4**). After preparing the salty solutions of each polymer for each formulation, salty CS solution was added to the corresponding salty CRG solution over stirring for 10 min. Later, the formed PECs were characterised by measuring size and ZP using Zetasizer, and turbidity ( $\lambda = 550 \text{ nm}$ ) using spectrophotometer.

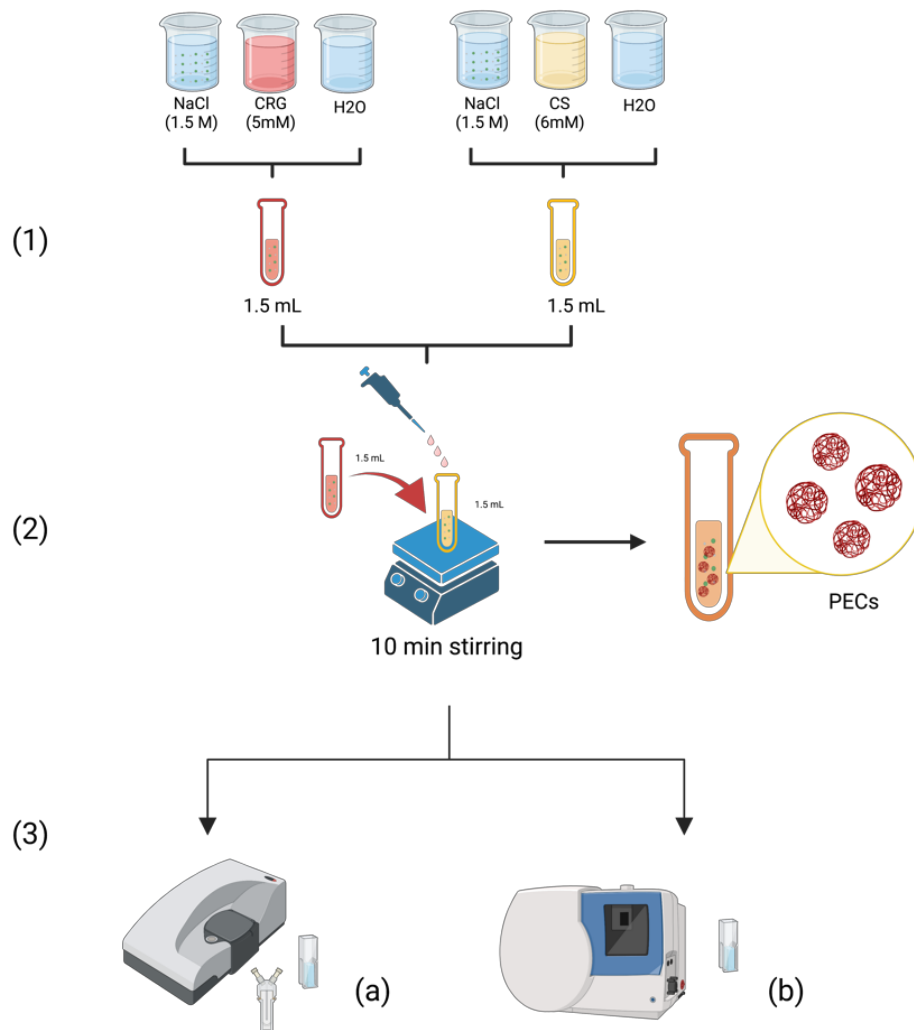


Figure 3.1 - The process of PECs formation (1 and 2) and characterisation (3). 1: preparing the PE solutions, 2: adding CRG to CS solution, and 3: characterisation using Zetasizer (a) and Spectrophotometer (b).

### 3.7 Method validation

Three points were selected for experimental testing. The points correspond to those with the most desired size and ZP values; the smallest size predicted by the design (284 nm) and ZP of |49| mV. Those values are illustrated in **Table 3.2** with the respective percentages and concentrations of PEs and NaCl.

Table 3.2 - Points selected from ED4 for validation. Desirability = 1 for all the predicted values.

Predicted value	Experimental concentrations			
	CS/ CRG/ NaCl Sum = 1	CS (mM)	CRG (mM)	NaCl (M)
ZP = -49 mV	0.12/ 0.65/ 0.25	0.357	1.631	0.0249
Size = 284 nm	0.66/ 0.1/ 0.23	1.996	0.247	0.0235
ZP = +49 mV	0.60/ 0.19/ 0.21	1.807	0.471	0.0209

Five replicas were prepared of each formulation, and size and ZP of PECs were measured as described previously.

### 3.8 Statistical analysis

In order to analyse the results obtained from the first study comparing PECs from two CRG sources, a two-tailed t-test with Welch's correction was performed to compare two groups. Analysis was conducted using GraphPad Prism Version 10.0.0 (131). Differences were considered significant when  $p < 0.05$ .

The ED used in this study is a D-optimal mixture experiments. It was constructed using Design Expert 6 (Stat-Ease Inc., MN, USA). It was carried out in the defined experimental region with a total of 15 runs. Mathematical models were used to fit the design. The regression mathematical model that guaranteed the best fit of the data to the design is the quadratic model and was used to relate the dependent variables (ZP and size) to the independent variables. The regression equations had the following format:

$$Y = \beta_1 * CS + \beta_2 * CRG + \beta_3 * NaCl + \beta_{12} * CS * CRG + \beta_{13} * CS * NaCl + \beta_{23} * CRG * NaCl$$

Polyelectrolyte Complexes from chitosan and carrageenan:  
optimization by Response Surface Methodology and method validation

Where  $\beta$ s are regression coefficients. In order to test the fit of the mathematical model to the ED, an ANOVA statistical analysis was carried out. The lack of fit was considered significant when  $p < 0.05$ .

## 4 Results and discussion

### 4.1 Preparation and characterisation of PECs from commercial CS and CRG

PECs from CS and CRG that could have a potential in future biomedical applications, namely in drug delivery and gene therapy, were prepared and characterized aiming at investigating the effects of CRG concentration and commercial origin on their characteristics. Upon adding CRG to CS solution, PECs were formed by a process called polyelectrolyte complexation. For polyelectrolyte complexation to happen, oppositely charged CS and CRG separate from the corresponding counterions and form ionic bonds with one another in an entropy-driven process (51,108–111).

The CRG used in this study is  $\kappa$ -CRG. It is a polyanion and is soluble only in hot water, therefore solution temperature was kept (20 - 60) °C to guarantee its maximum dissolution. Meanwhile, CS is soluble only in acidic conditions, and hereby, being dissolved in acetic acid. Filtration was the following pass to eliminate any undissolved residues in the PEs solution. Undissolved polymer residues can lead to biased readings of the measured parameters. Adding one solution to another should be under stirring. Therefore, the mixture of polymeric solutions in this study was stirred for 10 min to guarantee their formation. However, other studies have revealed that PECs form instantly and in less than 5  $\mu$ s (109).

PECs were characterized by measuring the size, PDI as an indication of size uniformity, and ZP. The registered values of the size and PDI of PECs (2/1 W/W to 6/1 W/W) prepared from two different CRG sources, *Biopolymer* and *Sigma*, are depicted in **Figure 4.1** and **Figure 4.2**, respectively. In addition, the values of ZP are depicted in **Figure 4.3**.

Despite all the results not being statistically significant, one can notice from **Figure 4.1** that size tends to decrease with the decrease of CRG concentration in the formulation, that is from 2/1 where there is the highest CRG concentration to 6/1 where there is the lowest CRG concentration. This result applies to both formulations from CRG *Biopolymer* and CRG *Sigma*. Similar results were obtained by Grenha et al and Rodrigues et al (130,131). This decrease might be related to less charge neutralisation when CS concentrations are much higher than the ones of CRG.

Moreover, precipitation took place in formulation 2/1 prepared with CRG *Sigma*. This precipitation can be attributed to charge neutralisation. The degree of neutralisation might be

associated with the quality of the PE; for example, commercial  $\kappa$ -CRG might be contaminated with other types of CRGs with different degrees of sulphation given that the degree of sulphation differs from one type to another (73). A study found that sulphation differences reflect in differences in the corresponding PECs. The same study found that a CRG with a higher degree of sulphation (x-CRG) had more tendency to form soluble PECs with CS than CRGs with a lower degree of sulphation ( $\kappa$ - and  $\beta$ -CRG) (132). This, in fact, can suggest that CRG from *Biopolymer* might be contaminated with CRGs with a higher degree of sulphation, or CRG from *Sigma* contaminated with CRGs with a lower degree of sulphation. In addition, this might be explained by charge distribution as it might not be uniform (130). Those results suggest that CRG from *Sigma* would exhibit a lower probability of generating precipitated formulations. Having a precipitated formulation from CRG *Sigma* encouraged us to use CRG *Biopolymer* in upcoming studies.

Regarding PDI (**Figure 4.2**), it also tends to decrease with decreased CRG concentration in both PECs *Sigma* and *biopolymer*, which might indicate that the smaller the particles are, the more homogenous the colloid is. Furthermore, there were no significant differences between the PECs *Biopolymer* and PECs *Sigma* as values varied between 0.246 (more homogeneous) and 0.783 (highly dispersed) in both (96).

ZP was measured to assess the surface charge and the stability of the colloidal systems. Although ZP values of PECs *Sigma* were slightly higher than those of PECs *Biopolymer*, this difference is not significant, as all the values were around +70 mV. This is inconsistent with the results observed by Grenha et al (131) or Rodrigues et al (130), as they found that the more CRG the formulation contains, the lower the ZP is, due to charge neutralisation. In general, all formulations exhibited values of ZP evidencing strongly cationic character. That property will also ensure excellent stability.

Polyelectrolyte Complexes from chitosan and carrageenan:  
optimization by Response Surface Methodology and method validation

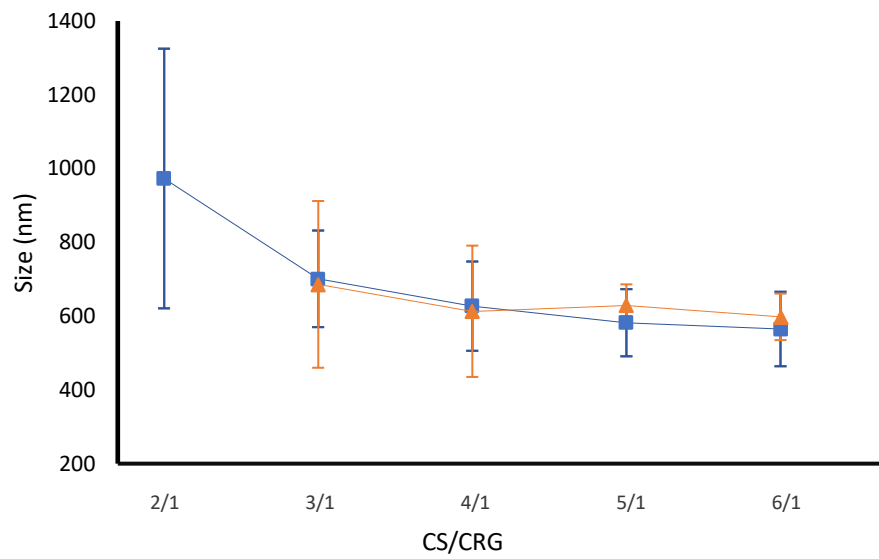


Figure 4.1 – Effect of CS/CRG mass ratios on the size of PECs produced with CS and CRG from *Biopolymer* (blue line) and *Sigma* (orange line); Formulation 2/1 *Sigma* precipitated (mean  $\pm$  SD, n = 3).

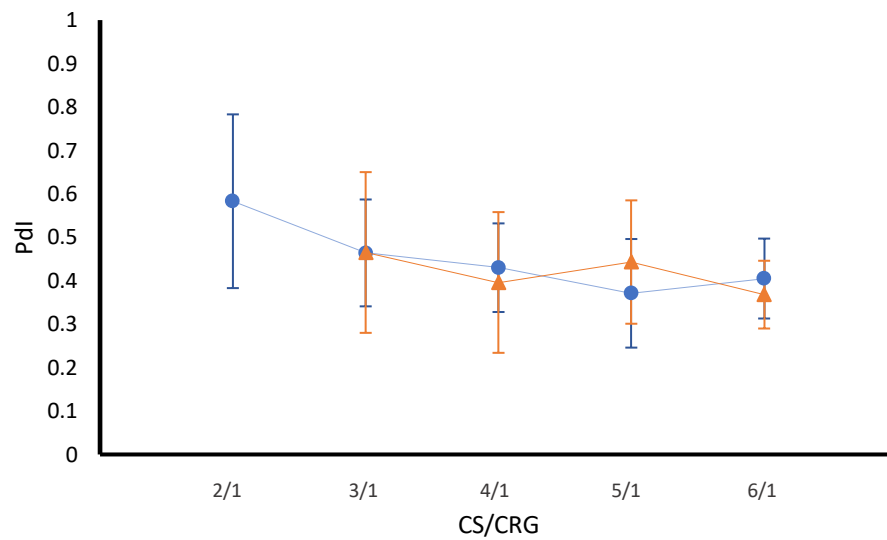


Figure 4.2 – Effect of CS/CRG mass ratios on the polydispersity index (PdI) of PECs produced with CS and CRG from *Biopolymer* (blue line) and *Sigma* (orange line); Formulation 2/1 *Sigma* precipitated (mean  $\pm$  SD, n = 3).

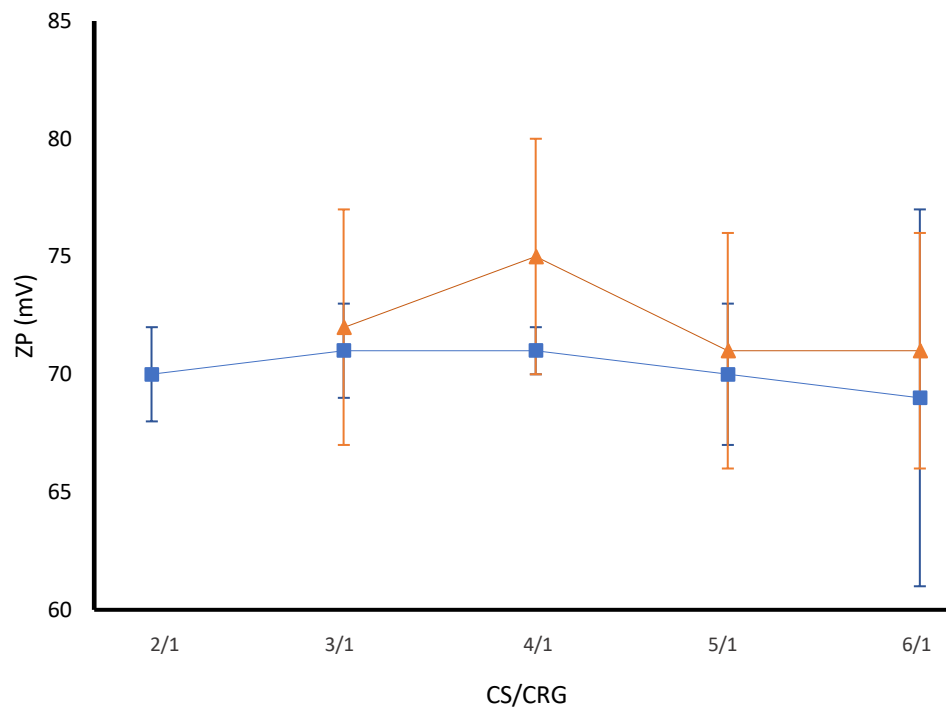


Figure 4.3 - Effect of CS/CRG mass ratios on the zeta potential (ZP) of PECs produced with CS and CRG from *Biopolymer* (blue line) and *Sigma* (orange line); Formulation 2/1 *Sigma* precipitated (mean  $\pm$  SD, n = 3).

## 4.2 Precipitation study, determining the solubility of PECs in salt solutions

PEs are very sensitive to their medium, especially to the ionic strength. The interaction of PEs with salts can lead to structural or physicochemical changes of those polymers and might also cause precipitation at a specific concentration (113,114,117). Bearing in mind the importance of PE-salt interaction either *in vivo* or *ex vivo* and the impact of salts on PECs formation, this precipitation study was conducted to investigate the precipitation of CS and CRG upon the addition of NaCl, CaCl<sub>2</sub>, and Na<sub>2</sub>SO<sub>4</sub>.

The study revealed that CRG did not precipitate at any concentration of the three salts. This, in fact, might be related to the dialysis quality of the PE, as the abrupt reduction of the dialysate pH to 3.19 during the dialysis might lead to alterations in PE's structural or physicochemical properties. The pH reduction might be related to microorganisms growth in the dialysis medium as our previous unpublished results showed that adding sodium azide, a biocide (133), to the dialysis medium can limit pH variation.

In the preparation process of CS solution, HCl (6 M) was added dropwise to the solution to guarantee CS solubility. CS did not dissolve in water since it was dialysed against water

instead of acid. Precipitation was noticed at NaCl ( $C_{final} = 2.79$  M), CaCl<sub>2</sub> ( $C_{final} = 1.05$  M), and Na<sub>2</sub>SO<sub>4</sub> ( $C_{final} = 0.78$  M). Those values correspond to CS concentrations of 0.55 mg/mL (2.22 mM), 0.99 mg/mL (3.99 mM) and 0.60 mg/mL (2.42 mM), respectively (**Table 4.1**). Precipitation took place due to a phenomenon called salting-out, which is defined as the precipitation of PEs in an aqueous solution induced by the addition of salts beyond their threshold concentration (134). This addition leads to the rearrangement of water molecules around salt ions instead of the solute, thus, stealing the water from solute, in this case CS.

Table 4.1 - NaCl, CS, and CRG concentrations at which precipitation happens.

<b>CS Precipitation concentration</b>	<b>NaCl</b>		<b>CaCl<sub>2</sub></b>		<b>Na<sub>2</sub>SO<sub>4</sub></b>	
	2.79 M		1.05 M		0.78 M	
	0.55 mg/mL	2.22 mM	0.99 mg/mL	3.99 mM	0.60 mg/mL	2.42 mM
<b>CRG Precipitation concentration</b>	No precipitation					

Those results suggest that the studied salts are classified as follows according to their salting-out capacities: Na<sub>2</sub>SO<sub>4</sub> > CaCl<sub>2</sub> > NaCl. This is only partially consistent with the Hofmeister series in the applied experimental conditions. According to the Hofmeister series, SO<sub>4</sub><sup>-</sup> > Cl<sup>-</sup> in salting-out capacity, which is verified in this study, and Na<sup>+</sup> > Ca<sup>2+</sup>; however, this does not apply here, as CaCl<sub>2</sub> reveals higher salting-out capability than NaCl. This might also be due to positive charge on the CS surface and its ability to form salts with the added ions (135,136). It can be concluded that Hofmeister series cannot be applied here given that it separates the effect of cation and anion.

The ultimate goal of this study is constructing an experimental design that predicts PECs physicochemical properties; thus, this precipitation study was built to restrict the concentrations on which the design will be built. However, the obtained results were not considered the maximums of the first experimental design shown in **Table 7.1**, as the refractory precipitation of CRG raised many concerns.

An additional pitfall of this study was not adjusting the pH of salts and polymers to the same value, which might strongly affect the final results. Given that CS turns insoluble at pH > 6, the addition of salt solution at neutral pH can influence its solubility and provoke

precipitation. In addition, ideally the dissolution of CS would have been carried out in acid instead of water. All this leads to unreliable results on the ionic strength impact. Of course, this might depend on other factors like deacetylation degree in the case of CS, molecular weight, and crystallinity (137).

### 4.3 Determining the isoelectric point (IP)

The IP is the point at which ZP of PECs is zero, thus the network charge of the colloidal system is zero (95). PECs precipitate when there is not enough charge for repulsion. This precipitation happens close to the IP. Therefore, determining the IP of PECs is crucial to avoid the concentrations of PEs that might provoke complex precipitates and agglomerations. For this reason, this part of our study investigated the point at which PECs from CS ( $M_n = 119$  kDa;  $M_w = 3216$  kDa) and CRG ( $M_n = 979$  kDa;  $M_w = 16420$  kDa) precipitate out of the solution.

PECs of 1/6 (CRG/CS) W/W to 10/1 (CRG/CS) W/W were generated which correspond to the charge ratios  $n^-/n^+ = 0.1 - 6.1$ . The polymer in default was always added to the polymer in excess to guarantee similar formation mechanisms (111). This explains adding CRG to CS in the formulations  $n^-/n^+ = 0.1 - 0.6$  and CS to CRG in the formulations  $n^-/n^+ = 1.2 - 6.10$ .

The characterisation of PECs was performed by measuring ZP and transmittance. It was found that ZP tends to decrease when  $n^-/n^+$  increases from 0.1 to 6.10 (**Figure 4.4**). This is expected as negative charge increases with increased CRG concentrations and ZP reaches its lowest value ( $-26$ ) where  $[SO_4^-]$  is 6 times  $[NRH_3^+]$ . However, surprisingly, ZP kept positive values in the formulations  $n^-/n^+ = 1.20$  to 1.65. At those points, one could expect either null values since the resulting complexes are nearly stoichiometric, or negative values as there are more  $[SO_4^-]$  than  $[NRH_3^+]$ . This, in fact, could be related to other factors such as the structural properties of CS and CRG. CRG is larger than CS and might coil up, meanwhile CS has a lower molecular weight and has a rigid structure (104). When CS is in default (acting as a guest) is added to CRG, the polymer in excess, (acting as a host), CRG can be crosslinked by CS molecules and wrapped in the core of the PEC. Then, the rest of CS molecules could remain on the surface imparting positive charge and some stability. This suggested mechanism is shown in **Figure 4.5**. In addition, due to the coiled structure of CRG, some of its charges are not accessible to interact with CS. Therefore, scrambled egg is the structural model that fits more here (103).

Polyelectrolyte Complexes from chitosan and carrageenan: optimization by Response Surface Methodology and method validation

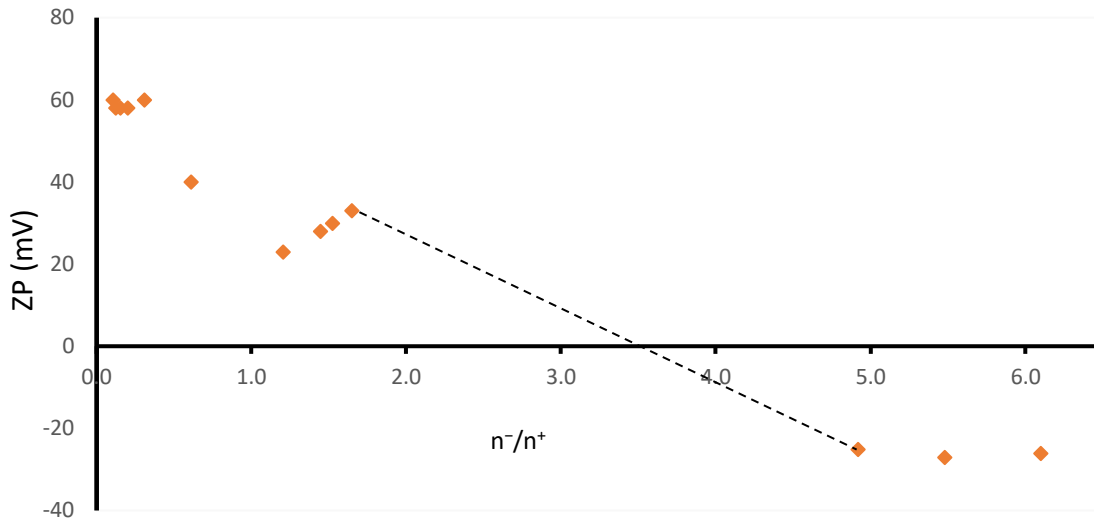


Figure 4.4 - Variation of zeta potential (ZP) values of PECs from CS and CRG with charge ratio ( $n^-/n^+$ ); From 1.80 to 4.33 precipitation was noticed and ZP was not measured.

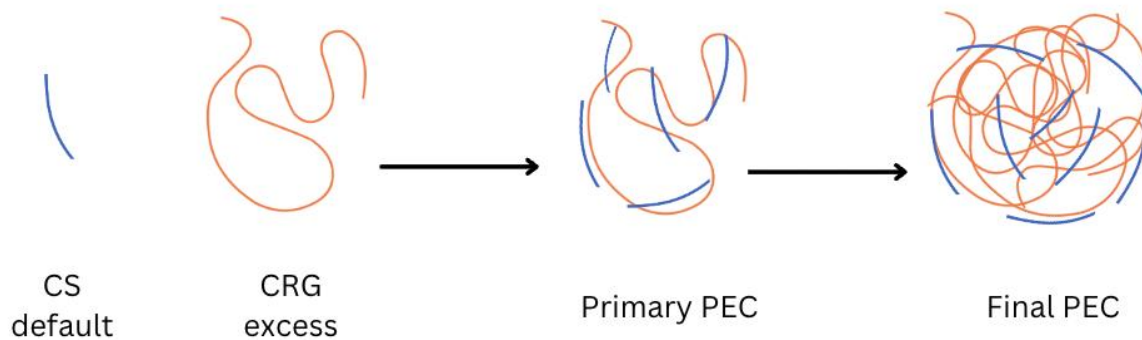


Figure 4.5 - The mechanism of PECs formation from CS and CRG.

By adding more CRG ( $n^-/n^+ = 1.80 - n^-/n^+ = 4.33$ ), CS in the solution is no longer enough to maintain on the surface and impart a positive charge. This leads to system neutralisation, followed by agglomeration and flocculation. This indicates that the IP is located somewhere in the range  $n^-/n^+ = 1.80$  to 4.33. Specifically, from the graph in **Figure 4.5**, it was estimated that the IP is achieved when  $n^-/n^+ \approx 3.5$ .

The IP is not achieved at  $n^-/n^+ = 1$ . This can be related to other factors besides structures and concentrations of the PEs. For example, in this study, it was theoretically assumed that each

CRG monomer carries one negative charge, since  $\kappa$ -CRG is used in this study and it carries only one sulphate group per monomer (**Figure 1.7**). However,  $\kappa$ -CRG might be contaminated with other CRG types. In addition, charge distribution might not be uniform. The bizarre values of ZP can also be related to the conditions where PECs were prepared such as temperature. Other studies showed that temperature influences the formation of PECs, either involving polypeptides (138) or polypeptide/synthetic polymer coacervate (139).

Besides ZP, transmittance is an important parameter to study the IP of PECs. Light is dispersed when it is forwarded to particles in suspension. Therefore, when light is directed to dispersed PECs, only a part of it will pass through the sample to the detector and is called transmitted light. Transmitted light is expressed in %T. Turbidity is the opposite of transmittance (turbidity = 1 – %T) as it increases with the decrease of transmitted. High turbidity values can indicate either a high yield of PECs or the presence of agglomerations (113,114,140).

In this study, transmittance was registered at  $\lambda = 550$  nm, as CS and CRG do not absorb at this wavelength. Transmittance variation with increased  $n^-/n^+$  is depicted in **Figure 4.6**. Those measurements were registered 2 - 3 h after PECs formation, therefore, formulations where aggregation was verified ( $n^-/n^+ = 1.80$  to  $4.33$ ) suffered precipitation. A study showed that PECs should be characterised up to one hour after their formation, otherwise, different bonds start forming (82). Therefore, %T = 0 was considered for formulations showing precipitation. That was supported by other studies where turbidity was found to hit the maximum in the aggregated formulations (113,138,141). In those studies transmittance values were registered immediately after PECs formation, while in the current study measurements were performed 1 - 3 h after their formation (141,142).

As shown in **Figure 4.6**, transmittance tends to decrease from the formulation 0.10 to the formulation 1.20. This is related to increased CRG charge concentrations and neutralisation which leads to more complex formation and turbidity. Unexpected increase in transmittance happened with further increase in  $n^-/n^+$  from 1.20 to 1.65. Further increase in CRG charge concentrations causes neutralisation and precipitation of PECs. This confirms the results obtained by ZP measures that the IP is located somewhere between  $n^-/n^+ = 1.80$  and  $4.33$ .

Transmittance values increase again from  $n^-/n^+ = 4.33$  to 6.10 as CRG charge concentration is 4 - 6 times the one of CS. Elevated transmittance values when the concentration

of one polymer significantly surpasses the other might either be related to the small size of PECs or to low yield.

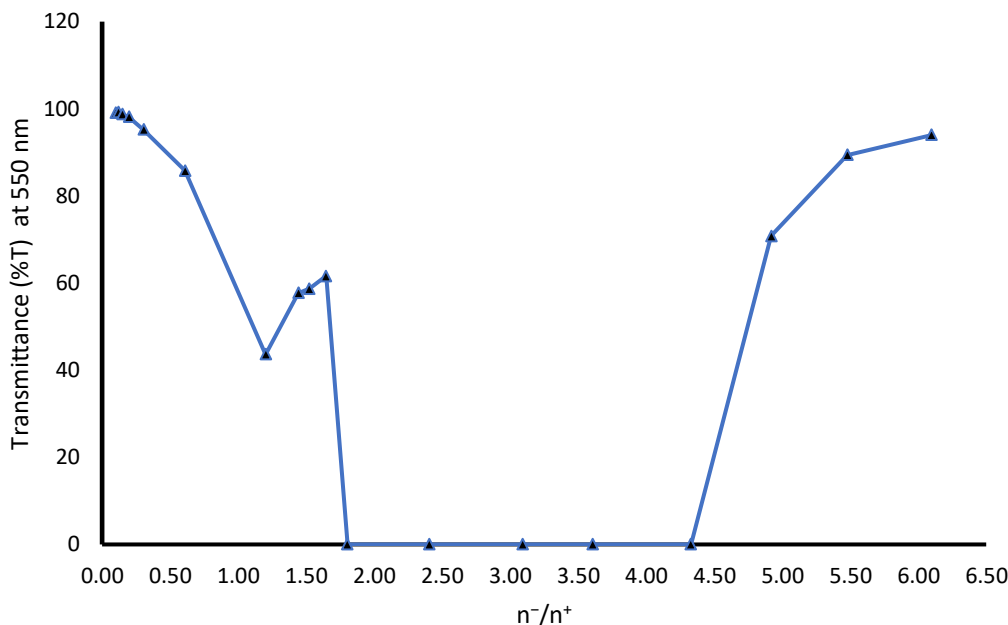


Figure 4.6 - Variation of transmittance (%T) of PECs from CS and CRG with charge ratio ( $n^-/n^+$ ).

#### 4.4 Constructing the Experimental Design (ED)

Four EDs representing the variations of PECs characteristics such as size, ZP, transmittance ( $\lambda = 500$  nm), and CR were built to reach to the ED4 that allowed us to obtain predictions with high desirability. All those four parameters are crucial to characterize NPs and PECs in order to investigate their applicability in industry or academia domains. As mentioned in previous sections, measuring turbidity can give indication of the yield of NPs. However, other parameters such as CR are measured to characterise the colloid. CR represents the number of photons arriving at the detector of Zetasizer per second and resulting from the intensity of scattered light after passing through the sample. The number of measurements made per second might also give indications about the yield. Therefore, an ED representing those factors was also constructed (111,143).

After building the ED4 (**Table 7.4**) on the range of  $CS_{max} = 2$  mM,  $CRG_{max} = 1.67$  mM,  $NaCl_{max} = 0.6$  M), response surfaces and contour diagrams representing size and ZP alterations as a function of CS, CRG, and NaCl concentration were built. Regarding turbidity and CR, the design was proven unable to provide quality predictions of those variables as lack of fit was

significant ( $p < 0.05$ ). Therefore, the corresponding response surfaces or contour diagrams are not illustrated.

One can notice that size variations (**Figure 4.7**) are related to the variations of the three parameters: CS, CRG and NaCl, altogether. Provided the properties of mixture designs (120), all the variables are interdependent with a sum of 100%, giving rise to varied size values.

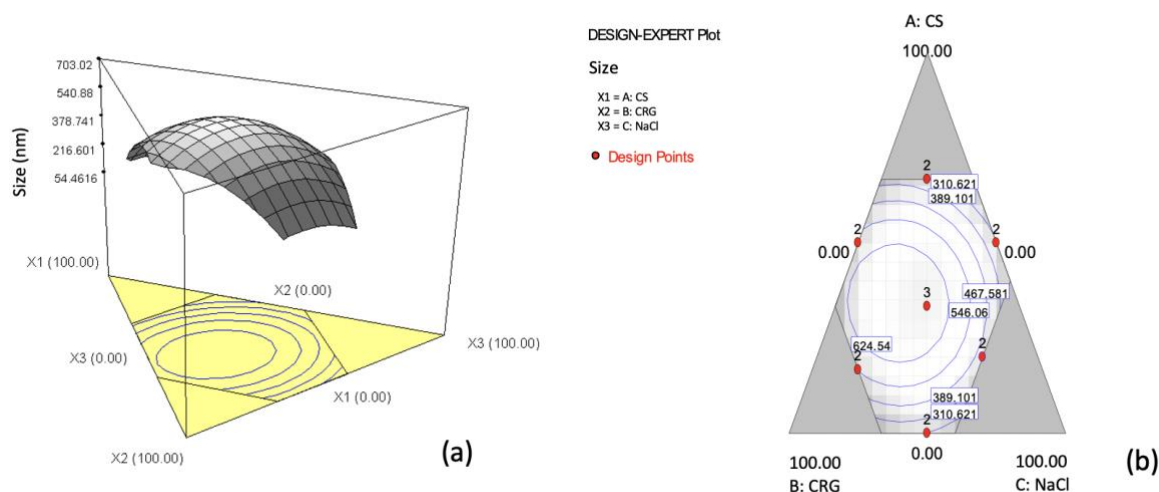


Figure 4.7 - Response surface (a) and contour diagram (b) of size.

Surface and contour diagrams (**Figure 4.7**) show that size hits the maximum ( $\sim 700$ ) nm when all the three components are added equally to the mixture, that is 30 - 40% of each, corresponding to CS, CRG and NaCl = 1 mM, 0.833 mM and 0.033 M, respectively. Therefore, it is recommended to avoid this region of the design with those concentrations if the purpose is preparing PECs for pharmaceutical applications to increase cellular uptake, potentiate cell interactions, promote absorption, or to deceive the immune response and avoid elimination, which requires lower sizes (138,142).

Size increases with the increment of CRG until reaching the maximum point, then decreases with a further increase in CRG contribution due to concomitant variations in NaCl and CS concentrations. The same applies to CS increment. When the concentration of one PE is much higher than the concentration of the other PE with opposite charge, less interactions take place and, thus, particles with smaller sizes are expected.

NaCl concentration was also found to influence size. From the contour diagram (**Figure 4.7-b**), it is noticed that increasing the portion of NaCl from the central point (1/3, 1/3, 1/3) up

(where NaCl is higher than 0.033 M) leads to decreasing the size. This may be due to the salting-out phenomenon where many polymers turn unable to react. On the other hand, this can be interpreted by improving PE chain flexibility (113,114). However, from (1/2, 1/2, 0) to (1/3, 1/3, 1/3), the effect is increasing the size from 570 nm to 700 nm. It is concluded that the effect of NaCl is dependent on the concentration of the other polymers, and it can have pros or cons effects.

The ED applies the regression equation below to predict size values:

$$\text{Size} = -7.33569 * \text{CS} - 0.56504 * \text{CRG} - 4.77292 * \text{NaCl} + 0.38941 * \text{CS} * \text{CRG} + 0.37087 \\ \text{CS} * \text{NaCl} + 0.22988 * \text{CRG} * \text{NaCl}$$

From this equation, one can notice that  $|\beta_1| > |\beta_3| > |\beta_2|$ , suggesting that CS is the main responsible for producing low-size PECs, followed by NaCl, and last by CRG (128). Since CS has lower molecular weight than CRG, it can be assumed that CS has a cross linking action. Therefore, having more CS might imply more cross linking, thus, smaller particles. Also, the synergistic blending effect is obviously obtained here (128) as mixing any two of the three components leads to a higher size compared with the pure compound, that is because  $\beta_{12}$ ,  $\beta_{13}$   $\beta_{23}$  have positive values. These results suggest that mixing only NaCl and one PE leads to the formation of some particles.

Deploying this ED, the smallest obtained size applicable in the medical domain is 284 nm; good enough to allow the passage of PECs, for instance, through the intestinal wall (32). That size can be obtained from different mixing ratios of the three components, but the most reliable one results from adding 66.62% CS, 9.90% CRG and 23.46% NaCl, that is 2 mM, 0.25 mM, and 0.023 M, respectively. However, 0.25 mM of CRG is considered a very low concentration that might not guarantee the formation of PECs, as despite the small size, the Tyndall effect was very weak to omitted when this formulation was prepared experimentally. Maybe an increase in CRG to at least 0.5 mM is required to make sure that PECs are formed. However, this is not possible once mixture designs put some restrictions such as the sum of all components must be equal to 1; an indication that factorial design is needed for further investigations in this region of the design (128).

Regarding ZP, CRG seems to have the highest influence on the parameter. From the surface diagram (**Figure 4.8-a**), ZP suffers a slight increase with increasing CRG concentrations until reaching the central point, where the opposite is just verified once ZP



is so small: 0.009, though), which may be due to a change in CS conformation and less exposure of positive charges. Same for CRG, as mixing only CRG and NaCl leads to PEC with higher ZP than of each separately due to folding consequences. Furthermore, mixing CS and CRG leads to higher ZP than the values obtained from each substance separately.

Moreover, the highest ZP that can be obtained from this design is  $\sim |49|$ . The ED4 is capable of suggesting several mixtures to obtain this value, but the most desirable ones are the following:

For ZP of +49 mV, CS, CRG, NaCl are 60.23%, 18.68%, 20.90% that corresponds to 1.8 mM, 0.47 mM, 0.02 M.

For ZP of -49 mV, CS, CRG, NaCl are 11.90%, 65.24%, 24.86% that corresponds to 0.36 mM, 1.63 mM and 0.02 M.

In the future, contour diagrams can be superimposed to obtain the desired features of size, ZP, and maybe turbidity. Also, many other parameters and factors should be taken into consideration in designing future studies. These include the molecular weight of the polymers, as well as their relative molecular weight. Interestingly, some studies found that polymers with larger molecular weight formed larger particles (84,103). Also, CS with different degrees of deacetylation can be used. Many other studies found that the size of PECs decreased with increasing the degree of deacetylation, thus, a higher degree of deacetylation can be considered in order to obtain smaller particles (114).

## 4.5 Method validation

In order to test the reliability of ED4, method validation was conducted on three points selected from the design. Mixtures predicted by the design has a high desirability. The results of ED4 validation are illustrated in **Table 4.2**.

Table 4.2 - Size, polydispersity index (PdI), zeta potential (ZP), and count rate (CR) values of PECs prepared for method validation (mean  $\pm$  SD, n = 5).

Predicted value	Experimental values			
	Size (nm)	PdI	ZP (mV)	CR
ZP = -49 mV	473 $\pm$ 18	0.212 $\pm$ 0.004	-50 $\pm$ 2	296 $\pm$ 66
Size = 284 nm	234 $\pm$ 7	0.288 $\pm$ 0.021	+38 $\pm$ 3	224 $\pm$ 12
ZP = +49 mV	378 $\pm$ 75	0.208 $\pm$ 0.105	+53 $\pm$ 3	222 $\pm$ 2

## Polyelectrolyte Complexes from chitosan and carrageenan: optimization by Response Surface Methodology and method validation

Regarding the first point, the value predicted by the design ( $-49$  mV) is located in the range from  $-52$  mV to  $-48$  mV obtained experimentally. However, the size of PECs of this formulation is close to  $500$  nm. Therefore, it is not considered a good elect for drug delivery.

On the other hand, the value predicted by the ED4 for the second point to validate the size ( $284$  nm) is not located in the range from  $227$  nm to  $241$  nm obtained experimentally, but it's very close to it. However, in all these replicas prepared for validation, the Tyndall effect was very weak to omitted. This, in fact, can be attributed to the extremely decreased CRG concentration ( $0.25$  mM) to  $2$  mM of CS; a great difference that justifies the presence of extra positive charges not reacted to negative ones. However, it is remarkable that the obtained size is smaller than that predicted by the design, which means that the designs could predict higher values than the real one. This formulation has also a  $ZP = +38$  mV  $\pm 3$ . This value is high enough to guarantee formulation stability.

Concerning the third point, the value predicted by the design ( $+49$  mV) is not located in the range from  $+50$  mV to  $+56$  mV obtained experimentally, but it is again very close to the lower extremity. The size obtained from this formulation is smaller than that obtained for the formulation with  $-49$  mV, but not as small as the desired  $284$  nm.

One can conclude from those results that the developed ED is considered valid, as despite having some values out of the considered range, they are not very far from its extremities, and this difference is not significant for this type of NPs.

Finally, further studies are highly needed to obtain more credible results once the degree of deacetylation, molecular weight, and length of the PE must be determined more accurately to retrieve good explanations of the results.

## 5 Conclusion

Owing to the physicochemical properties, high compatibility, and potential biodegradability of PECs compounded from many natural polymers like the ones used in this study, CS and CRG, they have great potential in medical applications, especially in drug delivery.

From this study, one can conclude about the sensitivity of PECs to several internal as well as external factors in the complexation reaction medium. Internal factors include concentration, Mw, and source of PEs, while external factors refer to the ionic strength of the solvent, and salt concentration. It was proven that the size and ZP of PECs from CS and CRG can be optimized by the addition of NaCl using RSM developed in this study. Afterwards, this method was also proven to be valid, and the design was found capable of predicting PECs as small as 284 nm and whose potential zeta is as high as |49| with a high desirability. Fortunately, those values represent NPs with promising medical applications in the future given that they can mediate cellular uptake and enhance absorption. Moreover, this method can be further improved to a potential future tool that helps researchers in academic or industry settings select the desired size and ZP of PECs, therefore, saving a great deal of time.

On the other hand, this design was unable to make quality predictions of the yield represented by the colloid's turbidity measurements. Numerous pitfalls must be avoided in constructing future designs which might be proven valid to make better predictions.

Ultimately, this study was subject to many obstacles, bearing in mind that it was intermittently conducted through different seasons of the year and given the sensitivity of PECs to temperature, this might be one of the many reasons for the reduced uniformity that should be avoided in the future. For the upcoming studies, it would be highly beneficial to study the PEs and analyse their characteristics more thoroughly before their application in formulating PECs. It would also be recommended to use the factorial design instead of mixture experiments given the limitations it posed to the study, especially since the sum of the factors should be equal to one.

## 6 References

1. ANSI [Internet]. [cited 2022 Aug 5]. ANSI NANOTECHNOLOGY STANDARDS PANEL (ANSI-NSP). Available from: <https://www.ansi.org/standards-coordination/collaboratives-activities/nanotechnology-panel>
2. WHO [Internet]. [cited 2022 Aug 5]. Addressing the impact of nanotechnology on health. Available from: <https://www.who.int/europe/activities/addressing-the-impact-of-nanotechnology-on-health>
3. NNI [Internet]. [cited 2022 May 8]. What Is So Special about “Nano”? Available from: <https://www.nano.gov/about-nanotechnology/what-is-so-special-about-nano>
4. Wang L, Hu C, Shao L. The antimicrobial activity of nanoparticles: present situation and prospects for the future. *International Journal of Nanomedicine*. 2017;12:1227–49.
5. Wagner V, Dullaart A, Bock AK, Zweck A. The emerging nanomedicine landscape. *Nature Biotechnology*. 2006;24(10):1211–7.
6. Raval N, Maheshwari R, Kalyane D, Youngren-Ortiz SR, Chougule MB, Tekade RK. Importance of Physicochemical Characterization of Nanoparticles in Pharmaceutical Product Development. In: *Basic Fundamentals of Drug Delivery*. Elsevier; 2019. p. 369–400.
7. Singh R, Lillard JW. Nanoparticle-based targeted drug delivery. *Experimental and Molecular Pathology*. 2009;86(3):215–23.
8. National Nanotechnology Initiative [Internet]. [cited 2022 Aug 5]. What’s So Special about the Nanoscale. Available from: <https://www.nano.gov/nanotech-101/special>
9. Brenner S. Nanomedicine: promises and challenges for the future of public health. *International Journal of Nanomedicine*. 2010;5:803–9.
10. Patra JK, Das G, Fraceto LF, Campos EVR, Rodriguez-Torres M del P, Acosta-Torres LS, et al. Nano based drug delivery systems: recent developments and future prospects. *Journal of Nanobiotechnology*. 2018;16(1):71.
11. Wagner V, Hüsing B, Gaisser S. *Nanomedicine: Drivers for development and possible impacts*. Seville: Institute for Prospective Technological Studies; 2008. Report No.: EUR 23494 EN.
12. PRECEDENCE RESEARCH [Internet]. [cited 2023 Nov 6]. Nanotechnology Drug Delivery Market Size, Report 2032. Available from: <https://www.precedenceresearch.com/nanotechnology-drug-delivery-market>
13. Ferlay J, Colombet M, Soerjomataram I, Parkin DM, Piñeros M, Znaor A, et al. Cancer statistics for the year 2020: An overview. *International Journal of Cancer*. 2021;Nanoparticles in Cancer Treatment: Opportunities and(4):778–89.

Polyelectrolyte Complexes from chitosan and carrageenan:  
optimization by Response Surface Methodology and method validation

14. McNamara K, Tofail SAM. Nanosystems: the use of nanoalloys, metallic, bimetallic, and magnetic nanoparticles in biomedical applications. *Physical Chemistry Chemical Physics*. 2015;17(42):27981–95.
15. Zahin N, Anwar R, Tewari D, Kabir MdT, Sajid A, Mathew B, et al. Nanoparticles and its biomedical applications in health and diseases: special focus on drug delivery. *Environmental Science and Pollution Research*. 2020;27(16):19151–68.
16. Thapa RK, Kim JO. Nanomedicine-based commercial formulations: current developments and future prospects. *J Pharm Investig*. 2023;53(1):19–33.
17. Rodríguez F, Caruana P, De La Fuente N, Español P, Gámez M, Balart J, et al. Nano-Based Approved Pharmaceuticals for Cancer Treatment: Present and Future Challenges. *Biomolecules*. 2022;12(6):784.
18. Waterhouse DN, Tardi PG, Mayer LD, Bally MB. A Comparison of Liposomal Formulations of Doxorubicin with Drug Administered in Free Form: Changing Toxicity Profiles. *Drug Safety*. 2001;24(12):903–20.
19. Mukherjee A, Waters AK, Kalyan P, Achrol AS, Kesari S, Yenugonda VM. Lipid–polymer hybrid nanoparticles as a next-generation drug delivery platform: state of the art, emerging technologies, and perspectives. *International Journal of Nanomedicine*. 2019;14:1937–52.
20. Viúdez A, Ramírez N, Hernández-García I, Carvalho FL, Vera R, Hidalgo M. Nab-paclitaxel: A flattering facelift. *Critical Reviews in Oncology/Hematology*. 2014;92(3):166–80.
21. Begines B, Ortiz T, Pérez-Aranda M, Martínez G, Merinero M, Argüelles-Arias F, et al. Polymeric Nanoparticles for Drug Delivery: Recent Developments and Future Prospects. *Nanomaterials*. 2020;10(7):1403.
22. Awasthi R, Roseblade A, Hansbro PM, Rathbone MJ, Dua K, Bebawy M. Nanoparticles in Cancer Treatment: Opportunities and Obstacles. *Current Drug Targets*. 2018;19(14):1696–709.
23. Salata O. Applications of nanoparticles in biology and medicine. *Journal of Nanobiotechnology*. 2004;2(3):6.
24. Thambirajoo M, Maarof M, Lokanathan Y, Katas H, Ghazalli NF, Tabata Y, et al. Potential of Nanoparticles Integrated with Antibacterial Properties in Preventing Biofilm and Antibiotic Resistance. *Antibiotics*. 2021;10(11):1338.
25. World Health Organization (WHO) [Internet]. [cited 2023 Jun 16]. WHO Coronavirus (COVID-19) Dashboard. Available from: <https://covid19.who.int/>
26. Eisenstein M. Nanotechnology offers alternative ways to fight COVID-19 pandemic with antivirals. *Nature Biotechnology*. 2021;39(10):1169–71.

27. Namiot ED, Sokolov AV, Chubarev VN, Tarasov VV, Schiöth HB. Nanoparticles in Clinical Trials: Analysis of Clinical Trials, FDA Approvals and Use for COVID-19 Vaccines. *International Journal of Molecular Sciences*. 2023;24(1):787.
28. Farnudian-Habibi A, Mirjani M, Montazer V, Aliebrahimi S, Katouzian I, Abdolhosseini S, et al. Review on Approved and Inprogress COVID-19 Vaccines. *Iranian Journal of Pharmaceutical Research*. 2022;21(1).
29. Colognato R, Park MVDZ, Wick P, De Jong WH. Interactions with the Human Body. In: Fadeel B, Pietroiusti A, Shvedova AA, editors. *Adverse Effects of Engineered Nanomaterials*. Elsevier; 2012. p. 3–24.
30. Gwinn MR, Sokull-Kluttgen B. Regulation and Legislation. In: Fadeel B, Pietroiusti A, Shvedova AA, editors. *Adverse Effects of Engineered Nanomaterials*. Elsevier; 2012. p. 97–117.
31. Abdellatif AAH, Abdullah Fahad Alsowinea. Approved and marketed nanoparticles for disease targeting and applications in COVID-19. *Nano Reviews*. 2021;10(1):1941–77.
32. Mitchell MJ, Billingsley MM, Haley RM, Wechsler ME, Peppas NA, Langer R. Engineering precision nanoparticles for drug delivery. *Nature Reviews Drug Discovery*. 2021;20(2):101–24.
33. Lu XY, Wu DC, Li ZJ, Chen GQ. Polymer Nanoparticles. In: Teplow DB, editor. *Progress in Molecular Biology and Translational Science*. Elsevier; 2011. p. 299–323.
34. Joshi MD, Patravale V, Prabhu R. Polymeric nanoparticles for targeted treatment in oncology: current insights. *International Journal of Nanomedicine*. 2015;1001.
35. Crucho CIC, Barros MT. Polymeric nanoparticles: A study on the preparation variables and characterization methods. *Materials Science and Engineering: C*. 2017;80:771–84.
36. Zielińska A, Carreiró F, Oliveira AM, Neves A, Pires B, Venkatesh DN, et al. Polymeric Nanoparticles: Production, Characterization, Toxicology and Ecotoxicology. *Molecules*. 2020;25(16):3731.
37. Deshmukh AS, Chauhan PN, Noolvi MN, Chaturvedi K, Ganguly K, Shukla SS, et al. Polymeric micelles: Basic research to clinical practice. *International Journal of Pharmaceutics*. 2017;532(1):249–68.
38. Cabral H, Miyata K, Osada K, Kataoka K. Block Copolymer Micelles in Nanomedicine Applications. *Chemical Reviews*. 2018;118(14):6844–92.
39. Ghezzi M, Pescina S, Padula C, Santi P, Del Favero E, Cantù L, et al. Polymeric micelles in drug delivery: An insight of the techniques for their characterization and assessment in biorelevant conditions. *Journal of Controlled Release*. 2021;332:312–36.
40. Jerkins GW, Pattar GR, Kannarr SR. A Review of Topical Cyclosporine A Formulations—A Disease-Modifying Agent for Keratoconjunctivitis Sicca. *Clinical Ophthalmology*. 2020;14:481–9.

Polyelectrolyte Complexes from chitosan and carrageenan:  
optimization by Response Surface Methodology and method validation

41. Mandal A, Gote V, Pal D, Ogundele A, Mitra AK. Ocular Pharmacokinetics of a Topical Ophthalmic Nanomicellar Solution of Cyclosporine (Cequa®) for Dry Eye Disease. *Pharmaceutical Research*. 2019;36(2):36.
42. Kalhapure RS, Suleman N, Mocktar C, Seedat N, Govender T. Nanoengineered Drug Delivery Systems for Enhancing Antibiotic Therapy. *Journal of Pharmaceutical Sciences*. 2015;104(3):872–905.
43. Yuan W, Wei J, Lu H, Fan L, Du J. Water-dispersible and biodegradable polymer micelles with good antibacterial efficacy. *Chemical Communications*. 2012;48(54):6857.
44. Dias AP, da Silva Santos S, da Silva JV, Parise-Filho R, Igne Ferreira E, Seoud OE, et al. Dendrimers in the context of nanomedicine. *International Journal of Pharmaceutics*. 2020;573:118814.
45. BioMelbourne Network Progressing BioIndustry [Internet]. [cited 2023 Aug 6]. Starpharma – DEP® docetaxel positive phase 1 results; phase 2 commences. Available from: <https://biomelbourne.org/starpharma-dep-docetaxel-positive-phase-1-results-phase-2-commences/>
46. Mignani S, Shi X, Rodrigues J, Roy R, Muñoz-Fernández Á, Ceña V, et al. Dendrimers toward Translational Nanotherapeutics: Concise Key Step Analysis. *Bioconjugate Chemistry*. 2020;31(9):2060–71.
47. Mendling W, Holzgreve W. Astodimer sodium and bacterial vaginosis: a mini review. *Archives of Gynecology and Obstetrics*. 2022;306(1):101–8.
48. Lee JS, Feijen J. Polymersomes for drug delivery: Design, formation and characterization. *Journal of Controlled Release*. 2012;161(2):473–83.
49. Mohanty A, Uthaman S, Park IK. Utilization of Polymer-Lipid Hybrid Nanoparticles for Targeted Anti-Cancer Therapy. *Molecules*. 2020;25(19):4377.
50. Muthukumar M. 50th Anniversary Perspective: A Perspective on Polyelectrolyte Solutions. *Macromolecules*. 2017;50(24):9528–60.
51. Gucht J van der, Spruijt E, Lemmers M, Cohen Stuart MA. Polyelectrolyte complexes: Bulk phases and colloidal systems. *Journal of Colloid and Interface Science*. 2011;361(2):407–22.
52. Meka VS, Sing MKG, Pichika MR, Nali SR, Kolapalli VRM, Kesharwani P. A comprehensive review on polyelectrolyte complexes. *Drug Discovery Today*. 2017;22(11):1697–706.
53. Rinaudo M. Polyelectrolytes Derived from Natural Polysaccharides. In: Naceur Belgacem M, Gandini A, editors. *Monomers, Polymers and Composites from Renewable Resources*. Elsevier; 2008. p. 495–516.
54. Scranton AB, Rangarajan B, Klier J. Biomedical applications of polyelectrolytes. In: Peppas NA, Langer RS, editors. *Biopolymers II*. Berlin, Heidelberg: Springer; 1995. p. 1–

Polyelectrolyte Complexes from chitosan and carrageenan:  
optimization by Response Surface Methodology and method validation

54. (Abe A, Benoit H, Cantow HJ, Corradini P, Dušek K, Edwards S, et al., editors. *Advances in Polymer Science*; vol. 122).
55. Zhao L, Skwarczynski M, Toth I. Polyelectrolyte-based platforms for the delivery of peptides and proteins. *ACS Biomaterials Science & Engineering*. 2019;5(10):4937–50.
56. Shah S, Eyler A, Tabandeh S, Leon L. Electrostatically driven self-assembled nanoparticles and coatings. In: Chung EJ, Leon L, Rinaldi C, editors. *Nanoparticles for Biomedical Applications*. Elsevier; 2020. p. 349–70.
57. Rinaudo M. Chitin and chitosan: Properties and applications. *Progress in Polymer Science*. 2006;31(7):603–32.
58. Ali A, Ahmed S. A review on chitosan and its nanocomposites in drug delivery. *International Journal of Biological Macromolecules*. 2018;109:273–86.
59. Hamman JH. Chitosan Based Polyelectrolyte Complexes as Potential Carrier Materials in Drug Delivery Systems. *Marine Drugs*. 2010;8(4):1305–22.
60. Mathur NK, Narang CK. Chitin and chitosan, versatile polysaccharides from marine animals. *Journal of Chemical Education*. 1990;67(11):938.
61. Mazeau K, Pérez S, Rinaudo M. Predicted Influence of *N*-Acetyl Group Content on the Conformational Extension of Chitin and Chitosan Chains. *Journal of Carbohydrate Chemistry*. 2000;19(9):1269–84.
62. Hartig SM, Greene RR, Dikov MM, Prokop A, Davidson JM. Multifunctional Nanoparticulate Polyelectrolyte Complexes. *Pharmaceutical Research*. 2007;24(12):2353–69.
63. Silva M, Calado R, Marto J, Bettencourt A, Almeida A, Gonçalves L. Chitosan Nanoparticles as a Mucoadhesive Drug Delivery System for Ocular Administration. *Marine Drugs*. 2017;15(12):370.
64. Prego C, Paolicelli P, Díaz B, Vicente S, Sánchez A, González-Fernández Á, et al. Chitosan-based nanoparticles for improving immunization against hepatitis B infection. *Vaccine*. 2010;28(14):2607–14.
65. Song H, Su C, Cui W, Zhu B, Liu L, Chen Z, et al. Folic Acid-Chitosan Conjugated Nanoparticles for Improving Tumor-Targeted Drug Delivery. *BioMed Research International*. 2013;2013:1–6.
66. Li J, Ma FK, Dang QF, Liang XG, Chen XG. Glucose-conjugated chitosan nanoparticles for targeted drug delivery and their specific interaction with tumor cells. *Frontiers of Materials Science*. 2014;8(4):363–72.
67. PubChem [Internet]. [cited 2022 Dec 27]. beta-Carrageenan. Available from: <https://pubchem.ncbi.nlm.nih.gov/compound/beta-Carrageenan>

68. Olatunji O, Kalia S. Aquatic Biopolymers: Understanding their Industrial Significance and Environmental Implications. Dehradun, India: Springer International Publishing; 2020. 124–32 p.
69. Borsani B, De Santis R, Perico V, Penagini F, Pendezza E, Dilillo D, et al. The Role of Carrageenan in Inflammatory Bowel Diseases and Allergic Reactions: Where Do We Stand? *Nutrients*. 2021;13(10):3402.
70. Carrageenan [Internet]. [cited 2023 Jun 22]. Available from: <https://www.drugs.com/inactive/carrageenan-208.html#:~:text=Carrageenan%20has%20been%20determined%20to,allow%20carrageenan%20in%20infant%20formulas>.
71. Bixler HJ. The carrageenan controversy. *Journal of Applied Phycology*. 2017;29(5):2201–7.
72. Liu J, Zhan X, Wan J, Wang Y, Wang C. Review for carrageenan-based pharmaceutical biomaterials: Favourable physical features versus adverse biological effects. *Carbohydrate Polymers*. 2015;121:27–36.
73. Necas J, Bartosikova L. Carrageenan: a review. *Veterinární Medicína*. 2013;58(4):187–205.
74. Kindness G, Long WF, Williamson FB. Enhancement of antithrombin III activity by carrageenans. *Thrombosis Research*. 1979;15(1–2):49–60.
75. Kindness G, Long WF, Williamson FB. Anticoagulant effects of sulphated polysaccharides in normal and antithrombin III-deficient plasmas. *British Journal of Pharmacology*. 1980;69(4):675–7.
76. Leibbrandt A, Meier C, König-Schuster M, Weinmüllner R, Kalthoff D, Pflugfelder B, et al. Iota-Carrageenan Is a Potent Inhibitor of Influenza A Virus Infection. *PLoS ONE*. 2010;5(12):14320.
77. Daniel-da-Silva AL, Ferreira L, Gil AM, Trindade T. Synthesis and swelling behavior of temperature responsive  $\kappa$ -carrageenan nanogels. *Journal of Colloid and Interface Science*. 2011;355(2):512–7.
78. Leong KH, Chung LY, Noordin MI, Onuki Y, Morishita M, Takayama K. Lectin-functionalized carboxymethylated kappa-carrageenan microparticles for oral insulin delivery. *Carbohydrate Polymers*. 2011;86(2):555–65.
79. Rodrigues S, Cordeiro C, Seijo B, Remuñán-López C, Grenha A. Hybrid nanosystems based on natural polymers as protein carriers for respiratory delivery: Stability and toxicological evaluation. *Carbohydrate Polymers*. 2015;123:369–80.
80. Silva FRF, Dore CMPG, Marques CT, Nascimento MS, Benevides NMB, Rocha HAO, et al. Anticoagulant activity, paw edema and pleurisy induced carrageenan: Action of major types of commercial carrageenans. *Carbohydrate Polymers*. 2010;79(1):26–33.

Polyelectrolyte Complexes from chitosan and carrageenan:  
optimization by Response Surface Methodology and method validation

81. Drugs.Com [Internet]. [cited 2022 Nov 27]. Carrageenan. Available from: <https://www.drugs.com/inactive/carrageenan-208.html>
82. Bhattarai A, Tribhuvan University. A Review on Polyelectrolytes (PES) and Polyelectrolyte Complexes (PECs). *International Journal of Engineering and Technical Research*. 2020;9(08):876–89.
83. Smedt SCD, Demeester J, Hennink WE. Cationic Polymer Based Gene Delivery Systems. *Pharmaceutical Research*. 2000;17:113–26.
84. Ragelle H, Vandermeulen G, Pr at V. Chitosan-based siRNA delivery systems. *Journal of Controlled Release*. 2013;172(1):207–18.
85. Mao S, Sun W, Kissel T. Chitosan-based formulations for delivery of DNA and siRNA. *Advanced Drug Delivery Reviews*. 2010;62(1):12–7.
86. Briones AV, Sato T. Encapsulation of glucose oxidase (GOD) in polyelectrolyte complexes of chitosan–carrageenan. *Reactive and Functional Polymers*. 2010;70(1):19–27.
87. Zhao M, Zacharia NS. Protein encapsulation via polyelectrolyte complex coacervation: Protection against protein denaturation. *The Journal of Chemical Physics*. 2018;149(16):163326.
88. Sikwal DR, Kalhapure RS, Rambharose S, Vepuri S, Soliman M, Mocktar C, et al. Polyelectrolyte complex of vancomycin as a nanoantibiotic: Preparation, in vitro and in silico studies. *Materials Science and Engineering: C*. 2016;63:489–98.
89. Cheow WS, Hadinoto K. Self-assembled amorphous drug–polyelectrolyte nanoparticle complex with enhanced dissolution rate and saturation solubility. *Journal of Colloid and Interface Science*. 2012;367(1):518–26.
90. Liu C, Xu H, Sun Y, Zhang X, Cheng H, Mao S. Design of Virus-Mimicking Polyelectrolyte Complexes for Enhanced Oral Insulin Delivery. *Journal of Pharmaceutical Sciences*. 2019;108(10):3408–15.
91. Selvamani V. Stability Studies on Nanomaterials Used in Drugs. In: Mohapatra SS, Ranjan S, Thomas S, editors. *Characterization and Biology of Nanomaterials for Drug Delivery*. Elsevier; 2019. p. 425–44.
92. Petzold G, Nebel A, Buchhammer HM, Lunkwitz K. Preparation and characterization of different polyelectrolyte complexes and their application as flocculants. *Colloid & Polymer Science*. 1998;276(2):125–30.
93. Gaikwad VL, Choudhari PB, Bhatia NM, Bhatia MS. Characterization of pharmaceutical nanocarriers: in vitro and in vivo studies. In: Grumezescu AM, editor. *Nanomaterials for Drug Delivery and Therapy*. Elsevier; 2019. p. 33–58.
94. Lunardi CN, Gomes AJ, Rocha FS, De Tommaso J, Patience GS. Experimental methods in chemical engineering: Zeta potential. *The Canadian Journal of Chemical Engineering*. 2021;99(3):627–39.

Polyelectrolyte Complexes from chitosan and carrageenan:  
optimization by Response Surface Methodology and method validation

95. Zeta potential - An introduction in 30 minutes [Internet]. Malvern; 2015 [cited 2022 Sep 10]. Available from: <https://www.research.colostate.edu/wp-content/uploads/2018/11/ZetaPotential-Introduction-in-30min-Malvern.pdf>
96. Kumar A, Dixit CK. Methods for characterization of nanoparticles. In: Nimesh S, Chandra R, Gupta N, editors. *Advances in Nanomedicine for the Delivery of Therapeutic Nucleic Acids*. Cambridge: Elsevier; 2017. p. 43–58.
97. Pate K, Safier P. Chemical metrology methods for CMP quality. In: Babu S, editor. *Advances in Chemical Mechanical Planarization (CMP)*. Elsevier; 2016. p. 299–325.
98. Phil Vincent. NanoFASE. [cited 2022 Dec 3]. Zeta potential. Available from: [http://nanofase.eu/show/zeta-potential\\_1273/](http://nanofase.eu/show/zeta-potential_1273/)
99. Stetefeld J, McKenna SA, Patel TR. Dynamic light scattering: a practical guide and applications in biomedical sciences. *Biophysical Reviews*. 2016;8(4):409–27.
100. Nimesh S. Tools and techniques for physico-chemical characterization of nanoparticles. In: *Gene Therapy*. 1st ed. Elsevier; 2013. p. 43–63.
101. Philipp B, Dautzenberg H, Linow KJ, Kötz J, Dawydoff W. Polyelectrolyte complexes — recent developments and open problems. *Progress in Polymer Science*. 1989;14(1):91–172.
102. Boddohi S, Moore N, Johnson PA, Kipper MJ. Polysaccharide-Based Polyelectrolyte Complex Nanoparticles from Chitosan, Heparin, and Hyaluronan. *Biomacromolecules*. 2009;10(6):1402–9.
103. Sæther HV, Holme HK, Maurstad G, Smidsrød O, Stokke BT. Polyelectrolyte complex formation using alginate and chitosan. *Carbohydrate Polymers*. 2008;74(4):813–21.
104. Schatz C, Domard A, Viton C, Pichot C, Delair T. Versatile and Efficient Formation of Colloids of Biopolymer-Based Polyelectrolyte Complexes. *Biomacromolecules*. 2004;5(5):1882–92.
105. Inamdar N, Mourya VK. Chitosan and anionic polymers – Complex formation and applications. In: Tiwari A, editor. *Polysaccharides: Development, Properties and Applications*. 1st ed. UK: Nova Science Publishers; 2010. p. 333–77.
106. Tripathi A, Melo JS, editors. *Advances in Biomaterials for Biomedical Applications*. Singapore: Springer Singapore; 2017. 48–51 p.
107. Müller M, editor. *Polyelectrolyte Complexes in the Dispersed and Solid State II*. Berlin, Heidelberg: Springer; 2014. 110–15 p.
108. Ou Z, Muthukumar M. Entropy and enthalpy of polyelectrolyte complexation: Langevin dynamics simulations. *The Journal of Chemical Physics*. 2006;124(15):154902.
109. Dautzenberg H. *Physical Chemistry of Polyelectrolytes*. Tsetska Radeva, editor. New York: Marcel Dekker; 2001. 743 p.

Polyelectrolyte Complexes from chitosan and carrageenan:  
optimization by Response Surface Methodology and method validation

110. Gärdlund L, Wågberg L, Norgren M. New insights into the structure of polyelectrolyte complexes. *Journal of Colloid and Interface Science*. 2007;312(2):237–46.
111. Müller M, Keßler B, Fröhlich J, Poeschla S, Torger B. Polyelectrolyte Complex Nanoparticles of Poly(ethyleneimine) and Poly(acrylic acid): Preparation and Applications. *Polymers*. 2011;3(2):762–78.
112. Kulkarni AD, Vanjari YH, Sancheti KH, Patel HM, Belgamwar VS, Surana SJ, et al. Polyelectrolyte complexes: mechanisms, critical experimental aspects, and applications. *Artificial Cells, Nanomedicine, and Biotechnology*. 2016;44(7):1615–25.
113. Perry S, Li Y, Priftis D, Leon L, Tirrell M. The Effect of Salt on the Complex Coacervation of Vinyl Polyelectrolytes. *Polymers*. 2014;6(6):1756–72.
114. Delair T. Colloidal polyelectrolyte complexes of chitosan and dextran sulfate towards versatile nanocarriers of bioactive molecules. *European Journal of Pharmaceutics and Biopharmaceutics*. 2011;78(1):10–8.
115. Mateescu MA, Ispas-Szabo P, Assaad E, editors. Chitosan-based polyelectrolyte complexes as pharmaceutical excipients. In: *Controlled Drug Delivery*. Elsevier; 2015. p. 127–61.
116. Nimesh S, Thibault MM, Lavertu M, Buschmann MD. Enhanced Gene Delivery Mediated by Low Molecular Weight Chitosan/DNA Complexes: Effect of pH and Serum. *Molecular Biotechnology*. 2010;46(2):182–96.
117. Dautzenberg H, Kriz J. Response of Polyelectrolyte Complexes to Subsequent Addition of Salts with Different Cations. *Langmuir*. 2003;19(13):5204–11.
118. Khuri AI, Mukhopadhyay S. Response surface methodology. *Wiley Interdisciplinary Reviews: Computational Statistics*. 2010;2(2):128–49.
119. Yolmeh M, Jafari SM. Applications of Response Surface Methodology in the Food Industry Processes. *Food and Bioprocess Technology*. 2017;10(3):413–33.
120. Balding DJ, Cressie NAC, Fitzmaurice GM, Johnstone IM, Molenberghs G, Scott DW, et al., editors. *Response Surface Methodology*. 3rd ed. Hoboken, New Jersey: John Wiley & Sons, Inc; 2009. 856 p.
121. Breig SJM, Luti KJK. Response surface methodology: A review on its applications and challenges in microbial cultures. *Materials Today: Proceedings*. 2021;42:2277–84.
122. Avalle M, Chiandussi G, Belingardi G. Design optimization by response surface methodology: application to crashworthiness design of vehicle structures. *Structural and Multidisciplinary Optimization*. 2002;24(4):325–32.
123. McCarthy DF, Gallagher E, Gormley TR, Schober TJ, Arendt EK. Application of Response Surface Methodology in the Development of Gluten-Free Bread. *Cereal Chemistry Journal*. 2005;82(5):609–15.

Polyelectrolyte Complexes from chitosan and carrageenan:  
optimization by Response Surface Methodology and method validation

124. Nazzal S, Khan MA. Response surface methodology for the optimization of ubiquinone self-nanoemulsified drug delivery system. *American Association of Pharmaceutical Scientists*. 2002;3(1):23–31.
125. Emami J, Hamishehkar H, Najafabadi AR, Gilani K, Minaiyan M, Mahdavi H, et al. Particle size design of PLGA microspheres for potential pulmonary drug delivery using response surface methodology. *Journal of Microencapsulation*. 2009;26(1):1–8.
126. Ko JA, Park HJ, Park YS, Hwang SJ, Park JB. Chitosan microparticle preparation for controlled drug release by response surface methodology. *Journal of Microencapsulation*. 2003;20(6):791–7.
127. Sabbagh F, Muhamad II, Nazari Z, Mobini P, Taraghdari SB. From formulation of acrylamide-based hydrogels to their optimization for drug release using response surface methodology. *Materials Science and Engineering: C*. 2018;92:20–5.
128. Montgomery DC. Design and analysis of experiments. 8th ed. Ratts L, editor. Hoboken, NJ: John Wiley & Sons, Inc; 2013. 730 p.
129. Malvern Panalytical [Internet]. 2018. Particle concentration measurements on the Zetasizer Ultra – How it works. Available from: <https://www.malvernpanalytical.com/en/learn/knowledge-center/technical-notes/tn180720particleconczetasizerhowto>
130. Rodrigues S, Costa AMR da, Grenha A. Chitosan/carrageenan nanoparticles: Effect of cross-linking with tripolyphosphate and charge ratios. *Carbohydrate Polymers*. 2012;89(1):282–9.
131. Grenha A, Gomes ME, Rodrigues M, Santo VE, Mano JF, Neves NM, et al. Development of new chitosan/carrageenan nanoparticles for drug delivery applications. *Journal of Biomedical Materials Research Part A*. 2010;92A(4):1265–72.
132. Volodko AV, Davydova VN, Glazunov VP, Likhatskaya GN, Yermak IM. Influence of structural features of carrageenan on the formation of polyelectrolyte complexes with chitosan. *International Journal of Biological Macromolecules*. 2016;84:434–41.
133. PubChem [Internet]. [cited 2023 Jul 16]. Sodium azide. Available from: <https://pubchem.ncbi.nlm.nih.gov/compound/Sodium-azide>
134. Zhang P, Alsaifi NM, Wu J, Wang ZG. Salting-Out and Salting-In of Polyelectrolyte Solutions: A Liquid-State Theory Study. *Macromolecules*. 2016;49(24):9720–30.
135. Okur HI, Hladílková J, Rembert KB, Cho Y, Heyda J, Dzubiella J, et al. Beyond the Hofmeister Series: Ion-Specific Effects on Proteins and Their Biological Functions. *The Journal of Physical Chemistry B*. 2017;121(9):1997–2014.
136. Lehoux J, Dupuis G. Recovery of chitosan from aqueous acidic solutions by salting-out: Part 1. Use of inorganic salts. *Carbohydrate Polymers*. 2007;68(2):295–304.

Polyelectrolyte Complexes from chitosan and carrageenan:  
optimization by Response Surface Methodology and method validation

137. Sogias IA, Khutoryanskiy VV, Williams AC. Exploring the Factors Affecting the Solubility of Chitosan in Water. *Macromolecular Chemistry and Physics*. 2010;211(4):426–33.
138. Priftis D, Tirrell M. Phase behaviour and complex coacervation of aqueous polypeptide solutions. *Soft Matter*. 2012;8(36):9396–405.
139. Priftis D, Megley K, Laugel N, Tirrell M. Complex coacervation of poly(ethyleneimine)/polypeptide aqueous solutions: Thermodynamic and rheological characterization. *Journal of Colloid and Interface Science*. 2013;398:39–50.
140. Mountain GA, Keating CD. Practical considerations for generation of multi-compartment complex coacervates. In: Keating K, editor. *Methods in Enzymology*. Elsevier; 2021. p. 115–42.
141. Deng SM, Li X. Formation of Polyelectrolyte Complexes Based on Pendant-Type Imidazolium Organosilicon Polymer with Poly(Sodium Acrylate). *Journal of Macromolecular Science, Part A*. 1997;34(4):695–704.
142. Rizvi SAA, Saleh AM. Applications of nanoparticle systems in drug delivery technology. *Saudi Pharmaceutical Journal*. 2018;26(1):64–70.
143. Ulf Nobbmann. Malvern Panalytical. [cited 2023 Jul 14]. Derived count rate – what is it? Available from: <https://www.materials-talks.com/derived-count-rate-what-is-it/#:~:text=In%20the%20Zetasizer%20a%20range,the%20optimal%20200%2D500kcps%20range.>

## 7 Annexes

The experimental points prepared to construct ED1, ED2, and ED3 are illustrated in (Table 7.1), (Table 7.2), and (Table 7.3), respectively.

Table 7.1 - Concentrations of CS, CRG, and NaCl used to construct the ED1, in addition to the corresponding Size, ZP, %T, and Count Rate readings; measurement was not done (-).

Sample number	CS/CRG/NaCl Sum = 1	CS (mM)	CRG (mM)	NaCl (M)	pH	Size (nm)	PDI	ZP (mV)	%T	Count Rate (Kcps)
1	1/0/0	0.75	0	0	2.71	763	0.696	+5	79.1	24.5
2	0/1/0	0	0.75	0	2.63	1436	0.911	-9	100.7	21.3
3	0/0/1	0	0	0.500	2.65	-	-	-34	100.6	24.6
4	0.5/0.5/0	0.375	0.375	0	2.62	251	0.229	+22	93.4	260.4
5	0.5/0/0.5	0.375	0	0.250	2.64	380	0.343	+17	100.3	94.4
6	0/0.5/0.5	0	0.375	0.250	2.66	478	0.469	-16	100.6	34.2
7	0.33/0.33/0.33	0.25	0.25	0.167	2.66	1295	0.743	-14	93.6	28.0
8	0.167/0.167/0.67	0.125	0.125	0.333	2.64	2324	0.798	-14	99.2	45.1
9	0.167/0.67/0.167	0.125	0.5	0.083	2.65	288	0.243	-33	99.5	191.9
10	0.67/0.167/0.167	0.5	0.125	0.083	2.65	243	0.237	+27	100.2	137.2

Table 7.2 - Concentrations of CS, CRG, and NaCl used to construct the ED2, in addition to the corresponding Size, ZP, %T, and Count Rate readings; measurement was not done (-), precipitation happened (\*).

Sample number	CS/CRG/NaCl Sum = 1	CS (mM)	CRG (mM)	NaCl (M)	pH	Size (nm)	PDI	ZP (mV)	%T	Count Rate (Kcps)
1	1/0/0	3	0	0	2.55	653	0.345	+28	99.6	52
2	0/1/0	0	3	0	2.62	484	0.562	-5	100.1	59
3	0/0/1	0	0	0.100	2.62	303	0.414	-	-	65
4	0.5/0.5/0	1.5	1.5	0	2.58	729	0.636	+39	27.9	164
5	0.5/0/0.5	1.5	0	0.050	2.58	316	0.466	+19	99.9	30
6	0/0.5/0.5	0	1.5	0.050	2.58	303	0.414	-6	99.9	65
7*	0.33/0.33/0.33	1	1	0.033	2.58	-	-	-	-	-
8	0.167/0.167/0.67	0.5	0.5	0.067	2.70	25460	0.817	+18	77.9	109
9	0.167/0.67/0.167	0.5	2	0.017	2.69	466	0.278	-47	89.1	147
10	0.67/0.167/0.167	2	0.5	0.017	2.63	344	0.181	+51	96.9	227

Polyelectrolyte Complexes from chitosan and carrageenan:  
 optimization by Response Surface Methodology and method validation

Table 7.3 - Concentrations of CS, CRG, and NaCl used to construct the ED3, in addition to the corresponding Size, ZP, %T, and Count Rate readings; measurement was not done (-), precipitation happened (\*).

Sample number	CS/CRG/NaCl Sum = 1	CS (mM)	CRG (mM)	NaCl (M)	Size (nm)	PDI	ZP (mV)	%T	Count Rate (Kcps)
1	1/0/0	3,0	0	0	375	0,55	+5	99,7	35
2	0/1/0	0	2,5	0	323	0,416	-18	99,9	22
3	0/0/1	0	0	0,100	-	-	-	-	-
4	0.5/0.5/0	1,5	1,25	0	601	0,453	+44	47,2	192
5	0.5/0/0.5	1,5	0	0.050	193	0,415	+12	100,1	23
6	0/0.5/0.5	0	1,25	0.050	273	0,448	-4	100,1	25
7	0.33/0.33/0.33	1	0,83	0.033	1708	0,915	+39	52,4	127
8*	0.167/0.167/0.67	0,5	0,42	0.067	-	-	-	-	-
9	0.167/0.67/0.167	0,5	1,67	0.017	537	0,234	+51	89,2	213
10	0.67/0.167/0.167	2	0,42	0.017	324	0,249	+46	96%	368

Polyelectrolyte Complexes from chitosan and carrageenan:  
optimization by Response Surface Methodology and method validation

The experimental points of ED4 are illustrated in (Table 7.4). NaCl concentration in the formulations 14 and 15 should be 0.06 M; However, due to a mistake in the calculations, these two formulations contained NaCl (0.02 M). This experiment is to be repeated in the future.

Table 7.4 - Concentrations of CS, CRG, and NaCl used to construct the ED3, in addition to the corresponding Size, ZP, %T, and Count Rate readings.

Sample Number	CS/CRG/NaCl Sum = 1	CS (mM)	CRG (mM)	NaCl (M)	Size (nm)	PDI	ZP (mV)	%T	Count Rate (Kcps)
1	0/0.5/0.5	0	1.25	0.05	332	0,457	-4	99,9	21
2	0/0.5/0.5	0	1.25	0.05	315	0,373	-7	100,1	28
3	0.5/0/0.5	1.5	0	0.05	311	0,461	+8	99,8	30
4	0.5/0/0.5	1.5	0	0.05	364	0,556	+8	99,9	26
5	0.5/0.5/0	1.5	1.25	0	615	0,418	+37	48,6	160
6	0.5/0.5/0	1.5	1.25	0	570	0,417	+46	50,9	150
7	0.67/0.167/0.167	2	0.42	0.017	321	0,28	+49	95,9	197
8	0.67/0.167/0.167	2	0.42	0.017	309	0,272	+48	96,9	188
9	0.167/0.67/0.167	0.5	1.67	0.017	525	0,207	-49	87,7	127
10	0.167/0.67/0.167	0.5	1.67	0.017	547	0,188	-48	87,9	397
11	0.33/0.33/0.33	1	0.833	0.033	703	0,465	+40	60	236
12	0.33/0.33/0.33	1	0.833	0.033	591	0,352	+45	65,5	236
13	0.33/0.33/0.33	1	0.833	0.033	755	0,44	+41	59,3	206
14	0.20/0.20/0.60	0.6	0.5	0.02	443	0.232	+45	84.2	408
15	0.20/0.20/0.60	0.6	0.5	0.02	378	0.211	+41	88.4	345